

Delineate Anything Flow: Fast, Country-Level Field Boundary Detection from Any Source

Mykola Lavreniuk^{a,b}, Nataliia Kussul^{b,c,d}, Andrii Shelestov^{b,d}, Yevhenii Salii^{b,d},*

Volodymyr Kuzin^{b,d}, Sergii Skakun^c, and Zoltan Szantoi^{a,e}

^aEuropean Space Agency, Frascati, 00044, Italy,

^bSpace Research Institute NASU-SSAU, Kyiv, 03187, Ukraine,

^cUniversity of Maryland, College Park, MD 20742, United States,

^dNational Technical University of Ukraine “Igor Sikorsky Kyiv Polytechnic Institute”, Kyiv, 03056, Ukraine

^eStellenbosch University, Stellenbosch, South Africa

Corresponding author:

Mykola Lavreniuk

European Space Agency*, Frascati, 00044, Italy

nick_93@ukr.net

* International Research Fellow

Highlights

- DelAnyFlow: resolution-agnostic method for large-scale field boundary mapping.
- DelAny model delivers >100% higher mAP and 400× faster inference than SAM2.
- FBIS-22M: largest benchmark with 673K images and 22.9M field instances (0.25–10 m).
- Produced a national-scale, topologically consistent field map of Ukraine in 2024.
- Outputs are analysis-ready and improve operational products in smallholder systems.

Abstract.

Accurate delineation of agricultural field boundaries from satellite imagery is essential for land management, crop monitoring, and agricultural statistics, yet existing methods often produce incomplete boundaries, merge adjacent fields, and struggle to scale. We present the Delineate Anything Flow (DelAnyFlow) methodology, a resolution-agnostic approach for large-scale field boundary mapping. DelAnyFlow combines the DelAny instance segmentation model, based on a YOLOv11 backbone and trained on the large-scale Field Boundary Instance Segmentation–22M (FBIS-22M) dataset, with a structured post-processing, merging, and vectorization sequence to generate topologically consistent vector boundaries. FBIS-22M, the largest dataset of its kind, contains 672,909 multi-resolution image patches (0.25–10 m) and 22.9 million validated field instances. The DelAny model delivers state-of-the-art accuracy with over 100% higher mAP and 400× faster inference than SAM2. DelAny demonstrates strong zero-shot generalization and supports national-scale applications: using Sentinel-2 data for 2024, DelAnyFlow generated a complete field boundary layer for Ukraine (603,000 km²) in under six hours on a single workstation. DelAnyFlow outputs significantly improve boundary completeness relative to operational products from Sinergise Solutions and NASA Harvest, particularly in smallholder and fragmented systems (0.25–1 ha). For Ukraine, DelAnyFlow delineated 3.75 M fields at 5 m and 5.15 M at 2.5 m, compared to 2.66 M detected by Sinergise Solutions and 1.69 M by NASA Harvest. Trained models, source code, and vector outputs are publicly available, ensuring reproducibility. This work delivers a scalable, cost-effective methodology for field delineation in regions lacking digital cadastral data, with direct applications to crop classification, agricultural statistics, food security, and integration into Group on Earth Observations Global Agricultural Monitoring Initiative (GEOGLAM) and various Food and Agriculture Organization of the

United Nations (FAO) monitoring programs. A project landing page with links to models, code, national-scale vector outputs, and additional resources is available at <https://lavreniuk.github.io/Delineate-Anything/>.

Keywords: field boundary delineation, instance segmentation, agricultural monitoring, deep learning, vectorization, multi-resolution satellite imagery, Earth intelligence.

1. Introduction

Agricultural parcels are the basic spatial unit for virtually every decision that links satellite observations to land-management practice or policy. At the technical level, per-field geometries enable crop-type and phenological mapping that is 8–12 percentage points more accurate than pixel-wise approaches, because spectral trajectories can be summarized over internally consistent management units (Graesser and Ramankutty, 2017). Field polygons also underpin yield-estimation frameworks: when Kang and Özdogan (2019) aggregated biophysical predictors to Landsat-scale parcels, positional errors of only a few meters produced biases approaching 0.4 t/ha for Midwestern maize, emphasizing how delineation accuracy propagates non-linearly into production statistics. Similar challenges have been documented in Ukraine, where underestimation of cropland burning has significant environmental and political consequences (Hall et al., 2021), and where satellite-based datasets have been used for war damage assessment (Kussul et al., 2023), land degradation monitoring and policy support (Kussul et al., 2017).

Political-economic considerations amplify these technical needs. In the European Union, more than €45 billion per year in Common Agricultural Policy (CAP) payments are distributed on an area basis. Recent qualitative work shows that remote-sensing-based parcel layers have become core instruments in an emerging “audit culture”, where paying agencies use automated boundary maps to flag suspicious claims and to direct costly on-the-spot controls (van der Velden et al., 2025). Nevertheless, large-scale benchmarks reveal that even state-of-the-art delineation models still leave 20–40% of parcels merged or fragmented (Waldner and Diakogiannis, 2020). Consequently, automatic outputs are now deployed mainly to quantify and reduce manual workload rather than to replace it outright within the Land Parcel Identification System (LPIS) (Erden et al., 2015).

The economic incentives extend beyond compliance. Accurate polygons enable precision-agriculture prescriptions whose profitability hinges on meter-level edge alignment; mis-registration along headlands can negate fertilizer savings and even damage water-course buffers (O'Connell et al., 2015). Financial services are likewise parcel-centric: insurers and banks increasingly bundle index-based products and credit lines with satellite yield forecasts that require clean, non-overlapping parcel geometries (North et al., 2019). At the national scale, boundary layers facilitate food-security monitoring and crisis response. Sadeh et al. (2025) show that a five-million-parcel map of Ukraine enabled rapid quantification of conflict-induced crop-area losses, guiding export-license policy in 2023–2024.

Against this backdrop, open data initiatives such as AI4Boundaries (d'Andrimont et al., 2023) and high-resolution, multi-sensor benchmarks (Graesser and Ramankutty, 2017) have catalyzed a new generation of resolution-agnostic, instance-segmentation models. Yet the political and economic stakes described above demand not only high pixel-level accuracy but also topological correctness, completeness and consistency across heterogeneous agro-ecologies.

Despite recent advances in semantic segmentation and the emergence of foundation models such as the Segment Anything Model (SAM), existing approaches face persistent challenges in the context of operational field boundary mapping. Semantic segmentation methods often produce incomplete or topologically invalid boundaries that require extensive post-processing to extract closed-field geometries. These pixel-wise models also struggle with field merging and boundary ambiguity, particularly in smallholder systems characterized by small, irregular, and densely clustered fields or spectrally heterogeneous landscapes. Meanwhile, foundation models like SAM exhibit systematic over-segmentation, frequently misclassifying roads, hedgerows, or water bodies as part of agricultural parcels, and their computational demands limit applicability at the national

scale. Although prompt engineering and multi-scale refinements have been proposed, these methods typically rely on additional supervision and still fall short in delivering high-confidence, instance-level delineations suitable for cadastral or policy use.

These limitations create a critical gap: there is no existing methodology capable of producing high-confidence, topologically consistent field boundary layers at national scale, using multi-resolution satellite imagery, in a manner that meets the accuracy, completeness, and robustness standards required for operational agricultural management.

In this study, we introduce a resolution-adaptive methodology for national-scale agricultural field boundary mapping that integrates the state-of-the-art *Delineate Anything* model (Lavreniuk et al., 2025b) within a scalable, operational framework. Building on deep-learning-based instance segmentation, the methodology is designed to accommodate multi-resolution satellite inputs while preserving topological correctness and spatial consistency across administrative boundaries. Beyond segmentation, we propose a rigorous, quality-controlled post-processing sequence that transforms raw instance masks into validated vector boundary layers. These analysis-ready boundary layers are suitable for both scientific research and operational applications, including policy monitoring, food security assessments, and subsidy auditing. By coupling high-performing instance segmentation model with robust post-processing logic, our approach delivers boundary products that meet the accuracy, completeness, and robustness requirements of large-scale agricultural management programs.

The rest of the paper is structured as follows. Section 2 reviews related work on field boundary delineation, including traditional computer vision techniques, semantic segmentation, hybrid approaches, and emerging instance segmentation and foundation models, as well as existing operational products and benchmark datasets. Section 3 describes the data and methods,

introducing the FBIS-22M dataset, the DelAny instance segmentation model, and the full DelAnyFlow methodology, including adaptive tiling, structured post-processing, cross-tile integration, and vectorization. Section 4 outlines the experimental design and evaluation strategy, including zero-shot generalization, dataset size, and resolution-impact analyses. Section 5 presents the results, highlighting the performance of DelAny and DelAnyFlow relative to baseline methods and operational products. Section 6 provides a discussion of methodological advances, limitations, and implications for agricultural monitoring and policy. Finally, Section 7 concludes with a summary of key findings and directions for future research.

2. Related Works

2.1. Traditional Computer Vision Approaches

Early field boundary delineation methods relied on classical image processing techniques that identify spectral and spatial discontinuities between adjacent agricultural parcels. Edge detection algorithms, including Canny, Sobel, and Laplacian of Gaussian operators, extract boundaries by locating abrupt transitions in pixel intensity or spectral reflectance (Turker and Kok, 2013). While computationally efficient, these methods exhibit fundamental limitations that restrict their operational utility. Their reliance on low-level features makes them highly susceptible to noise, illumination variations, and intra-field spectral heterogeneity, frequently resulting in fragmented or incomplete boundary segments (North et al., 2019).

Region-based segmentation techniques, such as watershed algorithms, region growing, multiresolution segmentation, graph-based methods, and Simple Linear Iterative Clustering (SLIC), attempt to address edge detection limitations by grouping spectrally homogeneous pixels into coherent objects (Yan and Roy, 2014; Watkins and van Niekerk, 2019; Wagner and Oppelt,

2020; Crommelinck et al., 2016; Graesser and Ramankutty, 2017). These methods typically produce closed geometries and demonstrate reduced sensitivity to noise compared to edge-based approaches. However, their performance depends critically on parameter optimization, particularly thresholds governing spectral similarity and minimum object size. Inadequate parameterization leads to under-segmentation in heterogeneous landscapes or over-segmentation in smallholder systems, where field boundaries are less distinct (Waldner and Diakogiannis, 2020).

The scalability limitations of traditional approaches stem from their requirement for extensive manual parameter tuning and supplementary data sources. Many implementations necessitate cropland masks or historical field boundaries to filter irrelevant edges, limiting their applicability in regions with sparse ancillary data (Rahman et al., 2019). These constraints motivated the exploration of data-driven approaches capable of learning optimal feature representations directly from imagery.

2.2. Deep Learning Semantic Segmentation Methods

Recent advances in deep learning have transformed field boundary delineation by enabling semantic segmentation architectures that learn hierarchical spatial and spectral features for per-pixel classification. Deep learning has also shown promise in other remote sensing tasks, including building extraction (Wang et al., 2022a), road extraction (Chen et al., 2022a), agricultural mapping (Lavreniuk et al., 2018) and general boundary detection (Xie and Tu, 2015; Bertasius et al., 2014; Lavreniuk, 2024; Liu et al., 2019). However, these methods primarily focus on semantic boundary detection, often requiring post-processing to form closed objects and lacking the ability to distinguish individual field instances.

In the context of agriculture, convolutional neural networks, particularly U-Net variants, have demonstrated superior performance over traditional approaches by automatically extracting relevant field boundary features from satellite imagery (Garcia-Pedrero et al., 2019). DeepLabV3+ has achieved accurate field extent and boundary localization through multi-scale feature fusion on high-resolution imagery (Du et al., 2019), while specialized architectures such as HRRS-U-Net have improved cropland segmentation accuracy by preserving fine spatial detail and incorporating attention mechanisms to address fragmentation in heterogeneous regions (Xie et al., 2023).

A wide range of architectures has been explored in this context. Fully convolutional networks (FCNs) were among the first deep learning models used for field boundary extraction, particularly in smallholder systems (Persello et al., 2023), with some efforts applying contour-closing heuristics or super-resolution techniques to refine outputs (Masoud et al., 2019). U-Net-based models have also been applied to crop-specific settings, such as rice paddy delineation (Wang et al., 2022b). Other variations include ResUNet-a (Diakogiannis et al., 2020) and architectures augmented with novel loss functions, such as the Residual and Recurrent Attention U-Net (R2AttU-Net) with Lovasz-Softmax loss (Seedz et al., 2024) or U-Net integrated with Kolmogorov–Arnold Networks (Cambrin et al., 2024).

Multi-task learning frameworks extend semantic segmentation by predicting complementary outputs, such as field boundaries, cropland extent, and distance-to-boundary maps, within a shared architecture (Diakogiannis et al., 2020). These models enhance structural consistency and resolve ambiguities near field edges by leveraging joint supervision. For instance, FracTAL ResUNet integrates distance-to-boundary channels with hierarchical watershed post-processing to yield more complete contours (Waldner et al., 2021). Building on this approach, subsequent work applied transfer learning with FracTAL ResUNet to smallholder farming

systems, demonstrating the adaptability of the distance-aware representation to new regions and agricultural contexts (Wang et al., 2022c). Similarly, dual-branch models such as FieldSeg-DA fuse edge detection and extent estimation backbones to generate coherent vector geometries (Liu et al., 2022).

Despite these advances, semantic segmentation approaches face fundamental limitations. Their pixel-wise prediction paradigm often produces incomplete or topologically invalid boundaries, requiring extensive post-processing to extract closed field polygons. Furthermore, commonly used boundary-based evaluation metrics are highly sensitive to minor misalignments and fail to penalize field merging errors that degrade performance in operational applications. These challenges have prompted a shift toward instance-level modeling of agricultural fields.

2.3. Hybrid and Composite Approaches

To address the limitations of standalone semantic segmentation models, particularly in fragmented or spectrally heterogeneous landscapes, hybrid approaches integrate deep learning with classical computer vision and unsupervised methods. These strategies enhance boundary continuity, improve topological coherence, and adapt more robustly across diverse agro-ecological settings. For example, convolutional neural networks have been combined with clustering algorithms such as DBSCAN and spectral clustering to delineate field extents from NDVI time series, reducing reliance on labeled data (Li et al., 2022). Other frameworks augment semantic segmentation with foundation models like SAM via prompt-guided fusion, leveraging both contextual and edge-based cues to refine delineation (Xie et al., 2025). The HS-FRAG toolkit combines edge detection and watershed segmentation to extract polygons from high-resolution multispectral imagery, demonstrating resilience in smallholder systems (Duvvuri and

Kambhammettu, 2023). Earlier efforts also explored fusing deep networks with adaptive graph-based growing contours, illustrating one of the first hybrid attempts to capture closed agricultural parcels using both learned features and shape priors (Wagner and Oppelt, 2020). Additionally, methods that incorporate morphological leveling, multiscale segmentation, and particle swarm optimization have shown improved spatial coherence and field integrity on very high-resolution data (Gopidas and Priya, 2022). These composite strategies provide a flexible, modular architecture that strikes a balance between generalization and precision. However, they often introduce additional computational complexity or require careful tuning, which has further motivated the shift toward instance-level modeling.

2.4. Instance Segmentation and Foundation Models

The transition from semantic to instance segmentation represents a paradigm shift toward explicitly detecting individual field objects rather than boundary pixels. Instance-level architectures such as Mask R-CNN and specialized frameworks like DASFNet have demonstrated promising results in extracting coherent agricultural parcels from high-resolution satellite imagery (Lv et al., 2020; Lu et al., 2022). These methods address the field-merging problem inherent in semantic approaches by treating each agricultural parcel as a distinct instance with closed boundaries.

More recent instance segmentation models from general computer vision, including Co-DETR (Zong et al., 2023), ViT-Adapter (Chen et al., 2022b), EVA (Fang et al., 2022), EVP (Lavreniuk et al., 2025a), and recent real-time YOLO variants (Khanam and Hussain, 2024; Wang et al., 2024), offer improved accuracy and inference efficiency in natural image tasks, but their application in agricultural settings remains limited due to the lack of domain-specific,

instance-annotated data. While such architectures offer design innovations, their transferability to field segmentation has not been systematically validated. Existing datasets (Aung et al., 2020; d'Andrimont et al., 2023; Persello et al., 2023; Wang et al., 2022c) are often limited in size and resolution (e.g., 10-m Sentinel-2).

The introduction of large-scale foundation models, particularly the Segment Anything Model (SAM) (Kirillov et al., 2023), has offered new possibilities for zero-shot field extraction without extensive training data requirements. SAM's impressive generalization capabilities across diverse image domains initially suggested potential for agricultural applications. However, direct application to field boundary detection reveals significant limitations (Chen et al., 2024; Huang et al., 2024; Tripathy et al., 2024). SAM exhibits systematic over-segmentation, incorrectly identifying non-agricultural features such as roads and forests as field boundaries, resulting in reduced precision. Additionally, the computational cost of SAM limits its scalability for large-area mapping applications.

Subsequent efforts have explored strategies to adapt SAM to remote sensing contexts, including prompt engineering (Osco et al., 2023; Ren et al., 2023), weakly supervised learning (Sun et al., 2024), and multi-scale processing (Huang et al., 2024). While these methods offer improvements in localized settings, they require additional information such as field-level prompts or weak labels, which are often unavailable in large-scale agricultural applications. Even with the release of SAM2, key challenges such as false-positive detection and reliance on handcrafted prompts persist (Ravi et al., 2024), suggesting fundamental limitations in zero-shot transferability for robust field boundary delineation.

2.5. Operational Field Delineation Products

Despite methodological advances, the translation into operational field boundary products remains limited. Most commercial solutions operate as proprietary systems with minimal technical disclosure. Companies such as Field Boundary (Spacenus), Leaf, MapMyCrop, Farmdok, DigiFarm, OneSoil, and EOSDA offer field delineation services primarily through Sentinel-2 imagery, claiming Intersection over Union (IoU) accuracies between 0.80 – 0.96. While these platforms are optimized for large-scale deployment and user accessibility, their reliance on undisclosed architectures and training regimes limits their utility for scientific benchmarking and comparative evaluation.

Among the notable exceptions providing open methodological detail, NASA Harvest (<https://www.nasaharvest.org/>) has developed a systematic approach that employs time-series analysis of PlanetScope imagery (a commercial, non-free dataset) to delineate field boundaries through edge detection algorithms. Their methodology combines NDVI-based and PCA-based approaches to identify edges that consistently recur throughout temporal sequences, resulting in the delineation of over 5 million agricultural fields across Ukraine for 2021–2023 (Sadeh et al., 2025). Similarly, Sinergise Solutions (<https://medium.com/sentinel-hub/parcel-boundary-detection-for-cap-2a316a77d2f6>) has deployed a deep neural network framework utilizing ResUNet-a architecture across more than 1 million square kilometers, incorporating Europe-wide normalization strategies and super-resolution techniques for operational field boundary mapping across multiple countries, including Ukraine, Germany, Hungary, Spain, Lithuania, and Canada.

The scarcity of publicly accessible field delineation products continues to hinder reproducibility and large-scale method validation across agro-ecological zones. Without open, standardized datasets derived from operational-scale efforts, it remains difficult to assess model generalizability, compare performance across regions, or build upon prior work. Addressing this

limitation will require greater emphasis on public releases of delineation outputs, documentation of processing workflows, and collaborative benchmarking initiatives.

2.6. Benchmark Datasets for Field Boundary Delineation

Development of generalizable and operational models has been challenged by the scarcity of large-scale, high-quality benchmark datasets. Most existing studies have relied on limited regional samples or synthetic labels, raising concerns about model robustness across diverse agro-ecological zones.

Several datasets have been developed to address this gap. The AI4SmallFarms dataset (Persello et al., 2023) includes 62 Sentinel-2 image chips only covering plots from Cambodia and Vietnam, annotated with over 439 thousand field instances. AI4Boundaries (d'Andrimont et al., 2023) significantly scaled up these efforts by integrating 55 thousand image patches at both 10 m and 1 m resolutions, resulting in approximately 2.5 million field instances across Europe. PASTIS (Garnot and Landrieu, 2021) and its extensions (PASTIS-R, PASTIS-HD) offer curated subsets of Sentinel-2, Sentinel-1, and SPOT 6-7 VHR imagery with ~ 124 thousand labeled field objects, designed to evaluate the resilience of field delineation models under cloud cover and across sensing modalities. The recently released Fields of the World dataset (Kerner et al., 2024b) further expands geographic and ecological diversity, comprising 1.63 million delineated fields across multiple continents from 70,484 Sentinel-2 image tiles. Nevertheless, the limited resolution range and scale of existing datasets restrict their suitability for operational applications.

2.7. Evaluation Methodologies and Metrics

Semantic segmentation models are typically assessed using pixel-level metrics such as overall accuracy, boundary F1-score, and IoU, as demonstrated in studies employing U-Net variants (Waldner and Diakogiannis, 2020; Tetteh et al., 2023). However, these metrics often fail to penalize topological errors, such as field merging or fragmentation. For example, pixel-based IoU may remain deceptively high when adjacent fields are incorrectly merged, while boundary IoU, although designed to capture edge alignment, is overly sensitive to small misalignments, yielding disproportionately low scores for errors that are inconsequential from an operational perspective.

To better capture instance-level structure and penalize field merging or fragmentation, several recent studies have employed object-based metrics such as mean Average Precision (mAP). Instance-based evaluation has been shown to be more robust in transfer learning settings and more sensitive to geometric and topological quality (Kerner et al., 2024b; Lavreniuk et al., 2025b).

A standard measure in object detection and instance segmentation tasks is the mean Average Precision (mAP) metric, which provides a single summary statistic of model performance by averaging the Average Precision (AP) values for each class across multiple Intersection-over-Union (IoU) thresholds:

$$mAP = \frac{1}{n} \sum_{k=1}^n AP_k$$

where n is the number of classes and AP_k is the average precision for class k . In the case where all instances belong to a single "field" class, this simplifies to the AP of that class.

AP itself is derived from the relationship between precision and recall, defined as:

$$Precision = \frac{TP}{TP + FP}, Recall = \frac{TP}{TP + FN}$$

where TP, FP and FN denote true positives, false positives, and false negatives, respectively. The Average Precision score is then computed as the area under the precision–recall curve, commonly using step-wise interpolation. Given a ranked list of n predictions sorted by confidence, it is defined as:

$$AveragePrecision (AP) = \sum_{k=1}^{n-1} [r(k) - r(k-1)] \times max(p(k), p(k-1))$$

where $r(k)$ and $p(k)$ are the recall and precision at threshold k , respectively.

The quality of instance overlap is measured using the Intersection over Union (IoU):

$$IoU = \frac{|P \cap G|}{|P \cup G|}$$

where P is the predicted mask and G is the ground truth. An instance prediction is considered a true positive if $IoU \geq \tau$, where τ is a predefined threshold.

3. Methods and Data

In this section, we present a novel remote sensing methodology for agricultural field boundary delineation developed to address the inherent limitations of traditional semantic segmentation approaches. We introduce the *Delineate Anything Flow* (DelAnyFlow) method, a comprehensive and resolution-agnostic approach for large-scale automated field boundary extraction. DelAnyFlow reformulates the field boundary delineation task as an instance segmentation problem, which more effectively mitigates boundary misalignments and reduces the merging of adjacent fields. The method integrates the custom-trained instance segmentation model *DelAny* with a systematic post-processing framework comprising adaptive tiling, morphological refinement, and cross-tile unification. The final outputs are delivered as analysis-ready vector

datasets of topologically consistent, non-overlapping field boundaries suitable for operational agricultural applications at regional to national scales (Figure 1).

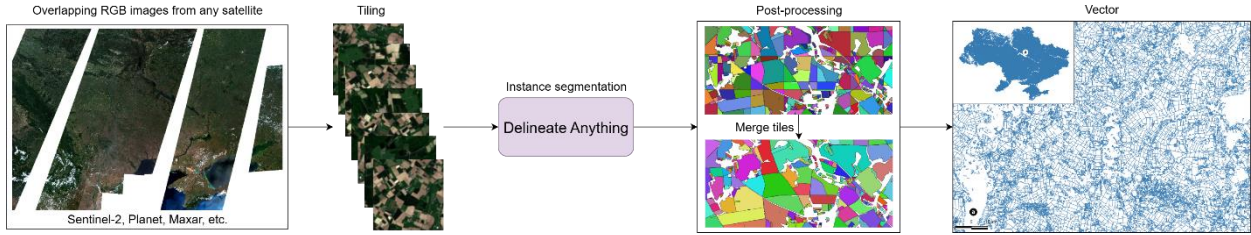


Figure 1. General workflow of the proposed scalable, resolution-agnostic *DelAnyFlow* methodology for national-scale field instance segmentation and boundary vectorization from multi-resolution satellite imagery. The methodology includes adaptive tiling, inference with the *Delineate Anything* model, post-processing to ensure topological consistency, and final vector boundary assembly.

3.1. Reframing Field Boundary Delineation as Instance Segmentation

Traditional semantic segmentation approaches for field boundary detection face persistent challenges, particularly when evaluated using boundary Intersection over Union (IoU). As illustrated in Figure 2, boundary IoU scores are highly sensitive to even minor spatial misalignments, despite predictions closely following ground truth boundaries. For example, a slight offset of only a few pixels can reduce the boundary IoU to 0.08 (Figure 2b), which disproportionately penalizes the model for an error with minimal impact on the usability of the boundary layer. In contrast, instance IoU remains robust under the same conditions, yielding a score of 0.98 (Figure 2e) by focusing on accurate delineation of entire field parcels rather than pixel-level alignment.

A more critical limitation of boundary IoU is its inability to adequately capture segmentation errors that result in the merging of adjacent fields into a single object. As illustrated in Figure 2, a partially detected boundary can yield a boundary IoU score as high as 0.93 (Figure 2c), despite the fact that multiple distinct fields have been incorrectly merged. In contrast, instance IoU more accurately reflects the severity of this error, with the score decreasing to 0.54 (Figure 2f). This discrepancy underscores the inadequacy of boundary IoU for agricultural applications, where maintaining the distinctness of individual fields is crucial for downstream tasks such as crop type classification, yield estimation, and the production of reliable agricultural statistics.

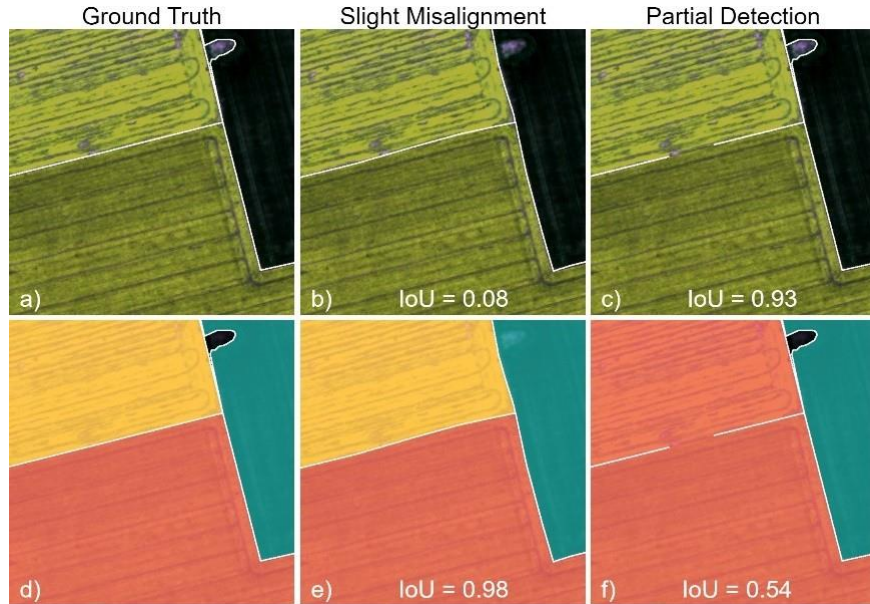


Figure 2: Comparison of task formulations and evaluation metrics for field boundary delineation. The top row illustrates field boundary masks (semantic segmentation), while the bottom row shows individual field masks (instance segmentation). Ground truth examples are shown in (a) and (d). Slightly misaligned boundaries result in a boundary IoU of 0.08 (b) and an instance IoU of 0.98 (e). Partially detected boundaries yield a boundary IoU of 0.93 (c) and an instance IoU of 0.54 (f).

To overcome these limitations, we reformulated the field boundary delineation task as an instance segmentation problem, where each field is treated as a distinct instance. The goal is to predict closed-field masks that inherently prevent boundary misalignment and field merging. These instance-level masks can be readily converted into boundary vectors using straightforward post-processing techniques such as contour extraction. This reformulation ensures that the evaluation metric (instance IoU) is fully aligned with the operational requirements of agricultural field mapping, enabling more consistent training and model assessment.

Instance IoU provides distinct advantages: it is less sensitive to minor boundary variations while appropriately penalizing critical errors such as the merging of adjacent fields, which can severely compromise data quality. By transitioning from semantic segmentation to an instance segmentation framework, this study advances the precision, reliability, and operational relevance of field boundary delineation. The resulting boundaries are both geometrically accurate and topologically distinct, thereby meeting the stringent quality standards required for large-scale agricultural monitoring and decision-support applications.

3.2. Field Boundary Instance Segmentation Dataset

Field delineation in agriculture remains challenging due to the high variability in field sizes, shapes, and image resolutions encountered across agro-ecological zones. While large-scale general computer vision datasets such as LAION-5B (5.85 billion images; Schuhmann et al., 2022) and SA-1B (1.1 billion instance masks; Kirillov et al., 2023) have enabled significant advances in other domains, available agricultural datasets for field delineation remain comparatively small. Existing datasets range from only 62 images in AI4SmallFarms (Persello et al., 2023) to

55 thousand images in AI4Boundaries (d'Andrimont et al., 2023), limiting the ability to train robust and generalizable models.

To address this limitation, we developed the Field Boundary Instance Segmentation-22M (FBIS-22M) dataset, the largest dataset currently available for agricultural field delineation. FBIS-22M comprises 672,909 high-resolution satellite image patches and 22,926,427 instance masks of individual fields, making it more than twelve times larger than the previously largest dataset, AI4Boundaries (d'Andrimont et al., 2023) (Table 1). To the best of our knowledge, FBIS-22M is also the first dataset to incorporate high-resolution imagery from commercial satellite platforms. This unique characteristic enhances its value for training models capable of delineating fields across diverse agricultural landscapes. FBIS-22M integrates imagery from multiple sensors, including

Sentinel-2

(https://www.esa.int/Applications/Observing_the_Earth/Copernicus/Sentinel-2), PlanetScope (<https://earth.esa.int/eogateway/missions/planetscope>), Maxar (<https://www.maxar.com/maxar-intelligence/products/satellite-imagery>), Pleiades (<https://earth.esa.int/eogateway/missions/pleiades>), and publicly available satellite sources, thereby providing a heterogeneous dataset that supports model development for a range of spatial resolutions and sensor modalities.

Table 1. Comparison of the FBIS-22M dataset with existing resources. The table contrasts FBIS-22M with large-scale general computer vision datasets and currently available agricultural field delineation datasets derived from satellite imagery, emphasizing the broader resolution range and larger scale of FBIS-22M.

Dataset	Resolution	# Images	# Instances
---------	------------	----------	-------------

General Computer Vision Datasets			
LAION-5B (Schuhmann et al., 2022)	-	5.85B	-
COCO (Lin et al. (2014))	-	330K	1.5M
Open Images (Kuznetsova et al., 2020)	-	998K	2.8M
SA-1B (Kirillov et al. (2023))	-	11M	1.1B
Field Boundary Delineation Datasets			
Farm Parcel (Aung et al., 2020)	10m	2K	-
India10K (Wang et al. (2022b))	-	-	10K
PASTIS (Garnot and Landrieu, 2021)	10m	2K	124K
PASTIS-R (Garnot et al., 2022)	10m	2K	124K
PASTIS-HD	1m & 10m	2K	124K
AI4SmallFarms (Persello et al., 2023)	10m	62	439K
AI4Boundaries (d'Andrimont et al., 2023)	1m & 10m	55K	2.5M
Fields of The World (Kerner et al., 2024a)	10m	70K	1.63M
FBIS-22M	0.25m-10m	673K	22.9M

FBIS-22M offers a broad range of spatial resolutions from 0.25 m to 10 m, covering both smallholder and large-scale agricultural applications. Specifically, the dataset includes images with resolutions of 0.25m, 0.3m, 0.5m, 1m, 1.2m, 2m, 3m, and 10m. This diversity in resolutions enables the accurate segmentation of both small, irregular fields as well as larger, expansive agricultural areas, supporting general FBIS-22M also provides significant geographic diversity, covering several European countries, including Austria, France, Luxembourg, the Netherlands, Slovakia, Slovenia, Spain, Sweden, and Ukraine (Figure 3). This broad geographic scope ensures that models trained on FBIS-22M can adapt to varied agricultural practices, land types, and environmental conditions. The dataset further demonstrates diversity in field densities, with images containing fewer than 10 fields to over 300 fields per image. This variability, illustrated in Figure 4, highlights its ability to represent both sparse and dense agricultural regions.

The construction of FBIS-22M prioritized quality and completeness. Official LPIS (Land Parcel Identification System) boundaries were utilized for most regions, while high-resolution commercial satellite imagery was manually annotated for regions where LPIS data was unavailable, such as Ukraine, ensuring full coverage. Similar to field-data collection protocols used in cropland mapping (Waldner et al., 2019), we ensured geographic and management diversity during sampling. Additionally, the dataset was manually cleaned by removing errors in field boundaries and inconsistencies to ensure accuracy.

The FBIS-22M dataset is divided into 636,784 training images and 36,125 test images, facilitating robust model development and statistically sound evaluation. As summarized in Table 1, FBIS-22M substantially exceeds the scale of existing agricultural field delineation datasets in both image count and the number of annotated field instances. By addressing this critical resource gap, FBIS-22M establishes a comprehensive benchmark for advancing precision agriculture and automated land parcel identification, positioning it alongside leading large-scale datasets in the broader computer vision community.

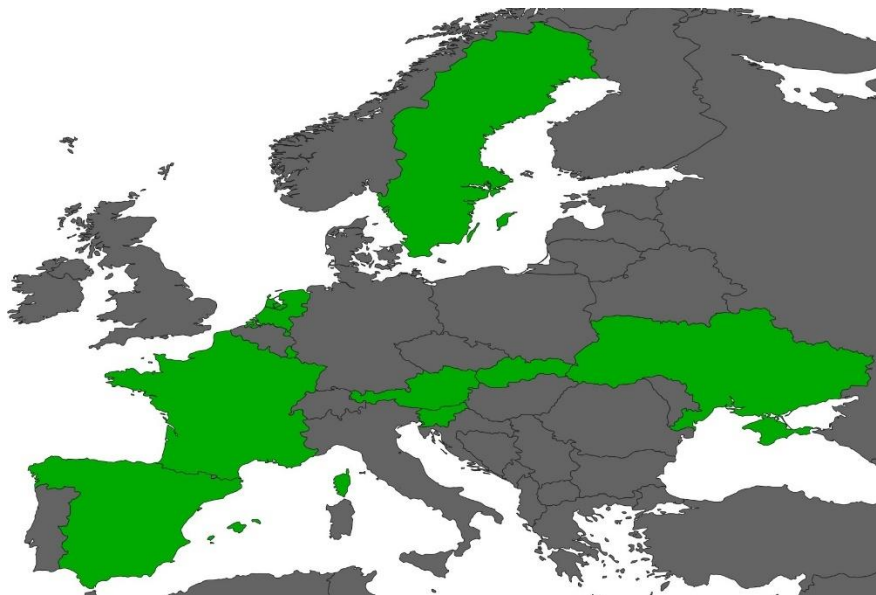


Figure 3: Geographic distribution of countries represented in the FBIS-22M dataset.

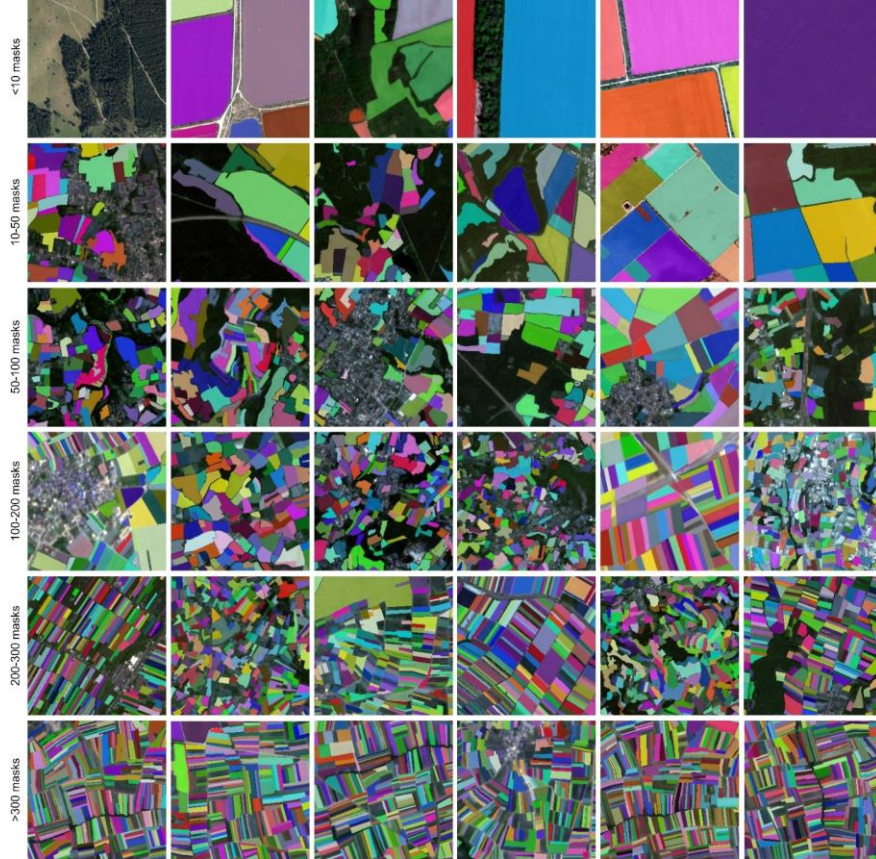


Figure 4: Examples of field boundary instance segmentation from our FBIS-22M dataset. The FBIS-22M dataset contains over 670K+ multi-resolution satellite images (ranging from 0.25m to 10m) and 22M+ field instance masks. Images are grouped by the number of fields to demonstrate the dataset’s diversity and scalability, and the challenge of separating fields across varying resolutions and geographies.

3.3. Instance-Based Field Segmentation with Delineate Anything

As the core deep learning component of the DelAnyFlow method, we developed the Delineate Anything (DelAny) model, a resolution-agnostic instance segmentation architecture

designed to extract agricultural field boundaries from satellite imagery (Lavreniuk et al., 2025b). Unlike traditional semantic segmentation models, DelAny formulates field delineation as an instance segmentation task, enabling the detection of individual fields and mitigating issues such as boundary merging and incomplete contours.

DelAny is based on the YOLOv11 instance segmentation architecture and is trained on the FBIS-22M dataset (Section 3.2), which supports generalization across different spatial resolutions, sensors, geographic regions, and seasonal conditions (Figure 5). No fine-tuning is performed at inference time; the model operates in a zero-shot setting, leveraging its generalization capability without retraining.

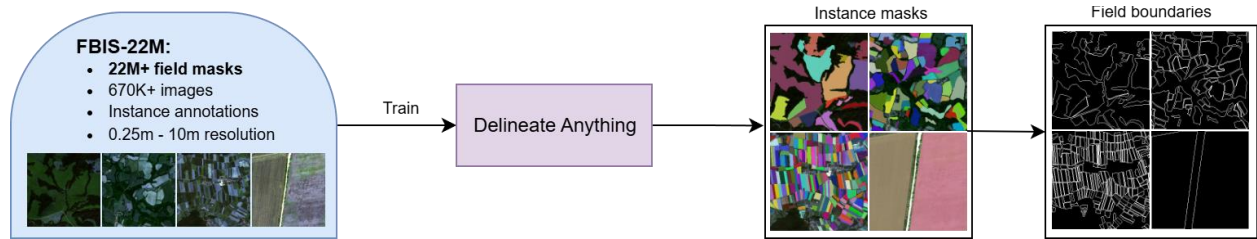


Figure 5: Workflow of the Delineate Anything model for field instance segmentation and field boundary extraction from arbitrary resolution satellite imagery, trained on our large-scale Field Boundary Instance Segmentation dataset (FBIS-22M), containing 22M field boundaries.

The model processes standardized 512×512 pixel RGB tiles and outputs instance masks and bounding boxes aligned to the tile dimensions. All predicted field instances are passed to the subsequent stages of DelAnyFlow without filtering to preserve full coverage across variable agricultural landscapes.

3.4. DelAnyFlow Overview

The DelAnyFlow methodology is a modular and resolution-agnostic approach designed to extract agricultural field boundaries from multi-sensor satellite imagery at large scale. The method is organized into five main stages (Figure 6):

1. **Adaptive data preparation and tiling.** Input imagery from different sensors and resolutions is preprocessed using resolution-aware tiling and overlap handling to ensure seamless coverage and compatibility with the instance segmentation model.
2. **Instance segmentation.** Each tile is processed with the DelAny instance segmentation model (Section 3.3), which predicts field-level instance.
3. **Structured post-processing.** Predicted masks are refined using geometric and morphological operations, including mask cleaning and area-based filtering, to remove artifacts and improve boundary definition.
4. **Cross-tile field unification.** Overlapping field instances from adjacent tiles are merged using spatial overlap and geometric criteria to ensure topologically consistent geometries across the entire area of interest.
5. **Vectorization and output generation.** Final raster masks are converted into analysis-ready vector polygons enriched with metadata.

DelAnyFlow is designed to scale efficiently from regional to national deployments while preserving boundary accuracy, completeness, and topological integrity. The resulting field boundary layers meet the requirements of operational applications such as agricultural monitoring, subsidy auditing, cadastral mapping, and food security analysis.

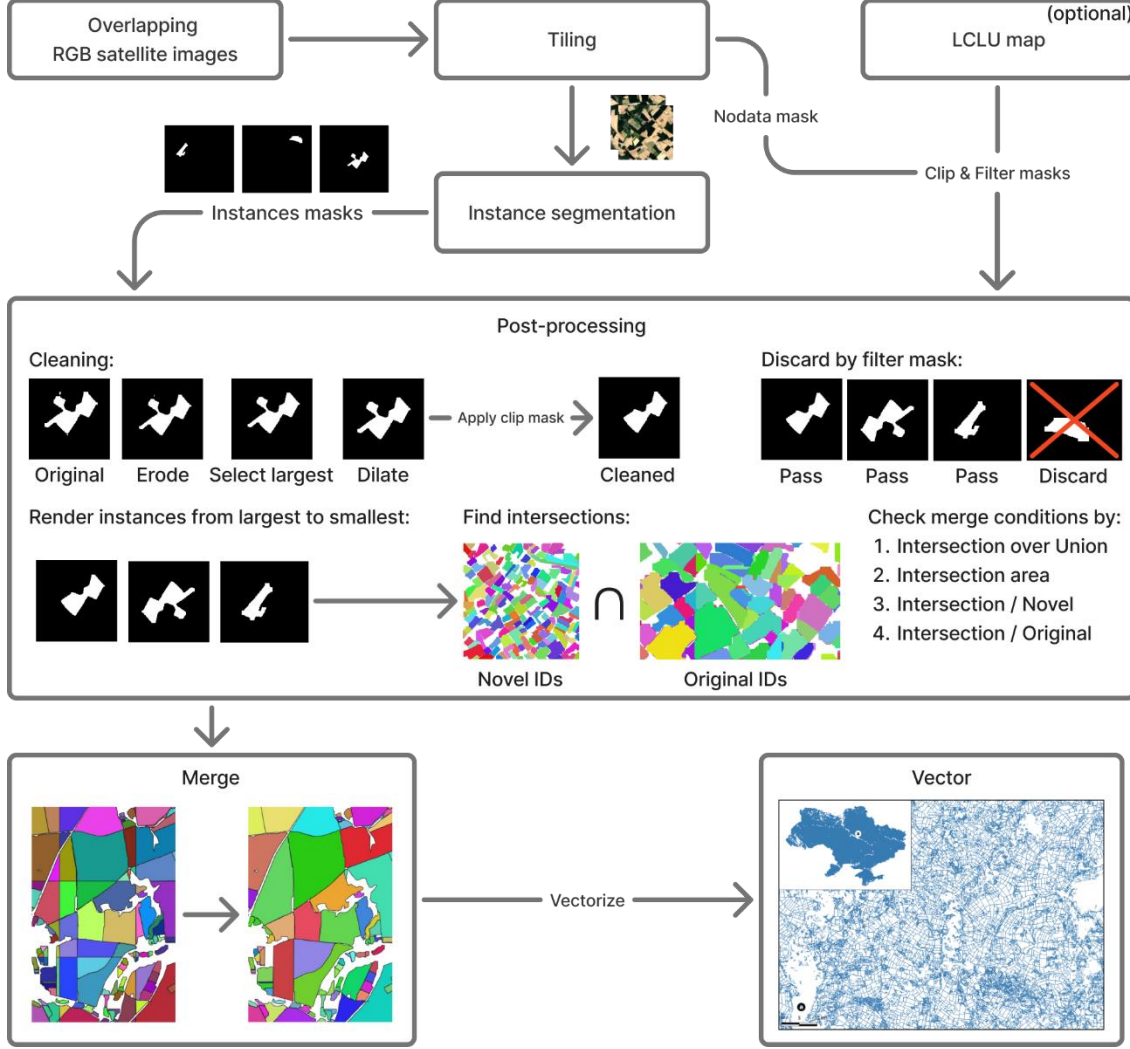


Figure 6: End-to-end workflow of the DelAnyFlow for large-scale field boundary delineation. The workflow supports diverse sensors and resolutions through adaptive tiling, robust instance segmentation, and multi-stage post-processing.

3.5. Output Integration and Final Boundary Generation

The post-processing stage of DelAnyFlow consists of a structured set of procedures designed to transform the raw instance segmentation outputs into topologically consistent, analysis-ready field boundary datasets. This stage addresses three primary challenges: (i) exclusion of detections in areas where the input data are incomplete or non-agricultural, (ii) removal of

artifacts and low-quality detections, and (iii) harmonization of overlapping field instances across tile boundaries.

To restrict delineation to valid agricultural areas, DelAnyFlow applies two levels of spatial masking. A primary quality mask excludes pixels flagged as missing or corrupted in the input imagery and removes areas classified as non-agricultural land cover (e.g., water, urban areas). A more conservative context mask, derived by expanding these exclusion zones, is used to identify areas adjacent to data gaps or linear features such as roads and forest edges, where boundary accuracy is typically reduced. These masks guide subsequent refinement operations and ensure that field boundaries are not extended into unreliable regions.

Field instances are prioritized in order of decreasing area, ensuring that larger and more distinct fields are retained first. Each instance then undergoes a hierarchical morphological refinement procedure to improve geometric quality:

1. Erosion is used to remove spurious single-pixel bridges or narrow connections that can incorrectly merge adjacent fields.
2. Connected-component analysis identifies and retains only the largest contiguous region, eliminating small, disconnected artifacts.
3. Dilation is applied to restore the corrected field mask to its original extent while maintaining improved topology.

This combination of erosion, connected-component filtering, and dilation is widely used in computer vision to correct segmentation artifacts and ensure that each retained field instance is a coherent, topologically valid object.

After morphological refinement, each instance is evaluated against quality criteria based on the proportion of valid pixels (derived from the quality masks) and minimum area thresholds. Instances failing these criteria are discarded before merging.

Because instance segmentation is applied independently to overlapping tiles, post-processing must resolve conflicts where multiple detections represent the same field. Overlapping instances are compared using IoU and area-based criteria. Merging occurs only when the overlap meets or exceeds empirically defined thresholds, which are designed to preserve larger, higher-confidence delineations while allowing fine-scale boundary refinements.

The refined tile-level masks are mosaicked into a single raster covering the full area of interest. Each field is assigned a unique identifier, and small artifacts below a minimum area threshold are removed. Finally, the raster is converted to vector polygons, which undergo topological validation and sliver removal. The resulting dataset contains non-overlapping, geospatially accurate field boundaries suitable for operational use in agricultural monitoring, cadastral mapping, subsidy auditing, and related applications.

4. Experimental Design and Evaluation Strategy

To comprehensively evaluate the proposed approach, we designed four experiments addressing different aspects of the field boundary delineation problem. Each experiment was intended to test a specific component of the methodology: (1) the effect of model configuration and training parameters on performance, (2) the ability of the model to generalize to unseen geographies and imaging conditions, and (3) the influence of dataset size and diversity on model accuracy. Together, these experiments provide a structured assessment of the DelAnyFlow method and its robustness across varying conditions.

4.1. Model Training

In the first experiment, we trained two versions of the DelAny model: the full version and a lightweight variant, DelAny-S. The full DelAny model uses the complete depth of the YOLOv11 architecture with a $1.5\times$ width multiplier and a maximum of 512 channels, resulting in 379 layers and 62 million parameters. In contrast, DelAny-S is configured with half the depth and one-quarter of the width (up to 1024 channels), yielding 203 layers and 2.9 million parameters.

Both models were trained for 30 epochs with a batch size of 320 (40 images per GPU) and a learning rate of 2×10^{-5} , using the standard YOLO loss function (Khanam & Hussain, 2024; Wang et al., 2024), which combines bounding box regression, objectness, classification, and task-alignment terms. Pre-trained COCO weights were used for initialization.

Training was performed on 8 NVIDIA H100 GPUs. To improve model generalization, we applied extensive data augmentation, including horizontal and vertical flipping, color jittering, mixup, and copy-paste augmentation. For the first 20 epochs, mosaic augmentation was also employed, consistent with standard YOLO training practices.

Model performance was evaluated using instance segmentation metrics from the Microsoft COCO evaluation protocol (Lin et al., 2014), namely mAP@0.5, which measures accuracy at a single Intersection-over-Union (IoU) threshold of 0.5, and mAP@[0.5:0.95], which averages the mean Average Precision (mAP) over ten IoU thresholds ranging from 0.5 to 0.95 in increments of 0.05. This evaluation framework captures both coarse and fine-grained geometric alignment of predicted field boundaries with the reference data.

4.2. Zero-Shot Cross-Region Generalization

In the second experiment, we evaluated the ability of the Delineate Anything models to generalize to geographic regions not included in the training data. Predictions were generated in a zero-shot setting, without any fine-tuning, for a diverse set of locations in various countries: Brazil, Cambodia, New Zealand, Rwanda, United States of America, Vietnam, and South Africa.

The aim was to assess robustness across different landscape structures, field sizes, and agricultural practices. Qualitative analysis focused on the model's ability to delineate fields with irregular shapes, varying textures, and complex spatial arrangements that differ from European agricultural systems (which dominate the training dataset).

4.3. Dataset Size Impact

The third experiment examined how the size and diversity of the training dataset influence model performance. We trained the Delineate Anything model on four datasets:

- AI4Boundaries (45K images)
- A 45K-image subset of FBIS-22M
- A 150K-image subset of FBIS-22M
- The full FBIS-22M dataset (636K images)

Performance was evaluated using the same instance segmentation metrics (mAP@0.5 and mAP@0.5:0.95). This experiment was designed to determine whether further dataset expansion would yield additional improvements or if accuracy begins to plateau at a certain scale. We also aimed to isolate the impact of dataset diversity (resolution, sensor types, geographic context) relative to size alone.

4.4. Data Spatial Resolution Impact

The fourth experiment focused on assessing how the spatial resolution of satellite imagery affects the model’s ability to detect agricultural fields. This analysis provides insight into whether higher-resolution imagery leads to improved delineation quality.

For this experiment, we performed field delineation on a 100 km² block within the Lvivska Oblast (Ukraine) using data from three different satellite sources: Sentinel-2, Planet, and Maxar. For Sentinel-2, we used the original imagery at 10 m resolution as well as data interpolated via cubic resampling to 5 m and 2.5 m resolution. For Planet, we employed its native 3 m per pixel imagery, while for Maxar, we utilized the original 2 m data and a pan-sharpened version with a spatial resolution of 50 cm.

5. Results

5.1. Quantitative and Qualitative Results

5.1.1. Performance Metrics and Benchmarking

Table 2 summarizes the performance metrics of the two modifications of *Delineate Anything* model and compares them with several state-of-the-art baselines, including MultiTLF (Kerner et al., 2024b), SAM (Kirillov et al., 2023), and SAM2 (Ravi et al., 2024). Of these, MultiTLF was re-trained on the FBIS-22M dataset to ensure a consistent evaluation framework.

Table 2. Quantitative performance comparison of field boundary delineation models on the FBIS-22M test set. The *DelAny* model and its lightweight variant (DelAny-S) are evaluated against several baseline approaches. † indicates model re-trained on the FBIS-22M dataset for consistency. Latency (ms) denotes the total inference time required to generate field boundaries for a 512 × 512-pixel patch on an NVIDIA A100 GPU. Best results are shown in bold.

Method	mAP@0.5	mAP@0.5:0.95	Latency (ms)
MultiTL [†]	0.257	0.110	55.8
SAM	0.339	0.197	13605
SAM2	0.382	0.235	10370
DelAny-S	0.632	0.383	16.8
DelAny	0.720	0.477	25.0

As shown in Table 2, DelAny achieves the highest scores in both mAP@0.5 and mAP@0.5:0.95 metrics, with the values of 0.720 and 0.477, respectively. These results surpass SAM2, the previous best-performing model, by 88.5% in mAP@0.5 and 103% in mAP@0.5:0.95. The lightweight version, DelAny-S, also outperforms SAM2 with gains of 65.5% in mAP@0.5 and 63% in mAP@0.5:0.95.

At the same time, both DelAny variants demonstrate significant computational advantages, being $415\times$ and $617\times$ faster than SAM2 in terms of average inference latency (ms) for DelAny and DelAny-S, respectively.

Figure 7 presents a qualitative comparison of the DelAny model with MultiTLF, SAM, and SAM2 across diverse agricultural landscapes. MultiTLF demonstrates strong performance in scenes characterized by large, sparsely distributed, and spectrally homogeneous fields but performs poorly in areas with densely packed small fields, frequently merging or omitting them. SAM and SAM2 exhibit a tendency to over-merge adjacent fields and to erroneously delineate non-agricultural features such as water bodies, grasslands, and forests, particularly in heterogeneous or non-agricultural settings. In contrast, DelAny maintains consistently high delineation accuracy across both sparse and dense field configurations and across a wide range of field sizes. Its instance-segmentation-based formulation provides a distinct advantage in detecting and correctly separating densely packed small fields.

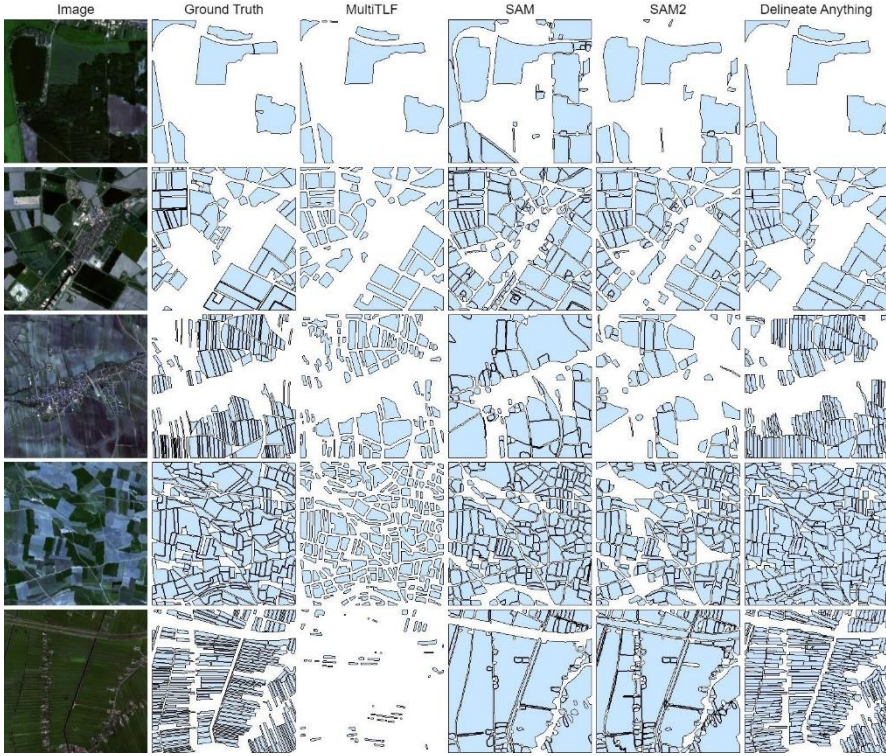


Figure 7: Qualitative results on the FBIS-22M test set. Delineate Anything is compared to MultiTLF Kerner et al. (2024b), SAM Kirillov et al. (2023), and SAM2 Ravi et al. (2024). For a fair comparison, the MultiTLF model was retrained using our FBIS-22M dataset. Different samples are carefully selected and presented, varying in size and density of the fields, to better illustrate the performance of each model under diverse conditions.

5.1.2. Zero-Shot Cross-Region Generalization

Figure 8 presents qualitative results of zero-shot predictions by the Delineate Anything models on previously unseen territories.

The segmentation results demonstrate that the model generalizes well to diverse landscapes, field patterns, and agricultural practices, including smallholder farms, large industrial fields, and varying crop arrangements. This shows strong robustness and potential for deployment

across different agro-ecological settings. The model consistently identifies field boundaries even under challenging conditions, such as irregular field shapes, varying textures, and diverse layouts.

5.1.3. Dataset Size Impact

Table 3 summarizes the performance of the Delineate Anything model when trained on datasets of varying size and diversity, including AI4Boundaries and subsets of FBIS-22M.

The results show a clear trend: increasing dataset size leads to improved performance. Training on a 45K-image subset of FBIS-22M yields a model with 0.597 mAP@0.5 and 0.335 mAP@0.5:0.95. Expanding to 150K images improves these metrics to 0.678 and 0.429, respectively. The best results, 0.720 mAP@0.5 and 0.477 mAP@0.5:0.95, are achieved when training on the full FBIS-22M dataset.

Notably, the model trained on 45K images from AI4Boundaries performs significantly worse than one trained on the 45K FBIS-22M subset, with 0.358 mAP@0.5 and 0.211 mAP@0.5:0.95 compared to 0.597 and 0.335, respectively.

These findings emphasize that, beyond dataset size, variation in resolution, sensor types, and geographic context is essential for achieving accurate and generalizable field boundary delineation.



Figure 8: Qualitative results of zero-shot predictions. Delineate Anything is applied to regions with different climates, terrains, and agricultural practices, highlighting its field delineation performance beyond the training data.

5.1.4. Data Spatial Resolution Impact

Figure 9 shows the delineation results of DelineateAnything on imagery from different sources. These results indicate that improvements in the spatial resolution of input data lead to more detailed delineation outputs, particularly for small fields. In Figure 9c–e, the overall structure of field boundaries remains consistent across all Sentinel-2 resolutions. However, applying 4× cubic interpolation significantly increases the detection of small private fields. At the same time, while Planet imagery (Figure 9f) has a slightly coarser resolution compared to interpolated Sentinel-2 data (Figure 9e) (3 m vs 2.5 m), its native resolution and higher image sharpness clearly enable more accurate delineation of field boundaries. In the case of Maxar imagery (Figure 9g–h), a substantial number of small fields can be detected; however, the delineation also exhibits a higher tendency to merge groups of adjacent small fields into a single polygon.

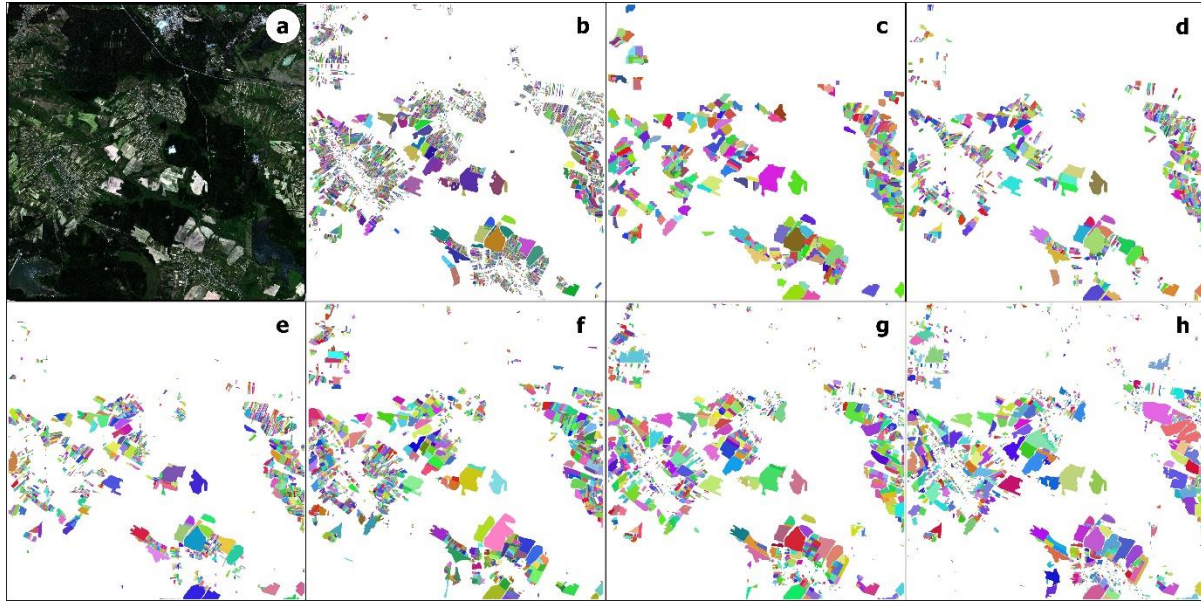


Figure 9: Comparison of fields delineation of 100 km sq. region in Lvivska oblast (coordinates of patch center: 23.3877, 49.8848) using satellite imagery with different spatial resolution. a — Maxar image; b — manually delineated fields; c — original 10m Sentinel-2; d — interpolated to 5m Sentinel-2; e — interpolated to 2.5m Sentinel-2; f — 3m Planet; g — 2m Maxar; h — pan-sharpened to 0.5m Maxar.

After manual verification of the scale at which polygon quality begins to deteriorate for the study fragment, the following thresholds and total detected field counts were obtained. For Sentinel-2 at 10 m and 5 m resolution, the area threshold was set at 0.5 hectares, resulting in 444 and 632 detected fields, respectively. For 2.5 m Sentinel-2 and Planet imagery, the threshold was 0.3 hectares, yielding 781 and 1038 fields. Maxar imagery allowed for the detection of fields as small as 0.1 hectares, with a total of 1120 fields, while pan-sharpened Maxar data further reduced the threshold to 0.05 hectares, resulting in 1516 polygons. For comparison, manual delineation produced 9468 fields, of which 8188 were smaller than 0.25 hectares and 9060 were smaller than 0.5 hectares.

Figure 10 presents the number of fields within logarithmically scaled area intervals. The results reveal a clear trend that the number of detected fields increases as the field size decreases. This confirms the improvement in detecting small fields when using higher-resolution data, even when obtained through interpolation. Additionally, the increased frequency of fields in the 10–70 ha range for Maxar data suggests that high-resolution imagery can sometimes lead to unnecessary merging of adjacent fields into larger groups.

Overall, this experiment demonstrates that using higher-resolution satellite data is advantageous for producing detailed delineation maps. However, even in the absence of very high-resolution imagery, Sentinel-2 data interpolated to 2.5 m performs only slightly worse than Planet data.

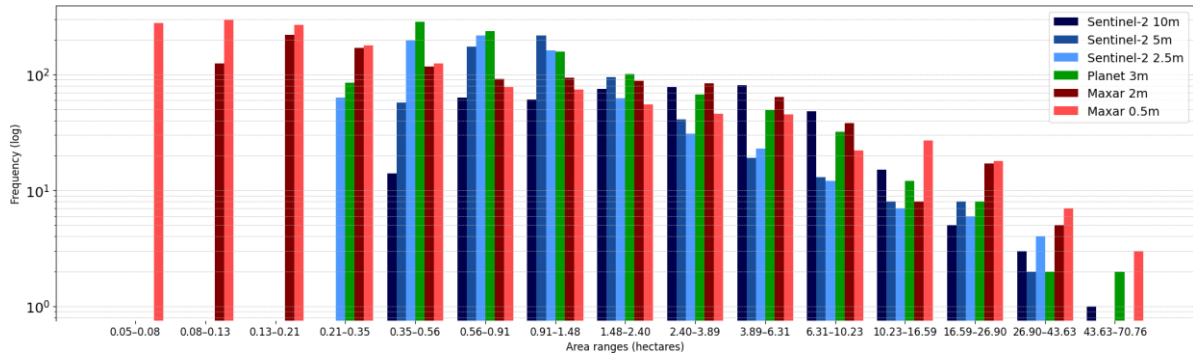


Figure 10: Distribution of the number of detected fields within different area ranges on input data with different sensors and spatial resolution.

Table 3. Impact of dataset size and diversity on model performance. Performance comparison of the DelAny model trained on the AI4Boundaries dataset and on different-sized subsets of FBIS-22M, highlighting the effect of dataset scale and diversity. Best results are in bold.

Dataset	# Images	mAP@0.5	mAP@0.5:0.95
---------	----------	---------	--------------

AI4Boundaries	45K	0.358	0.211
FBIS-22M (subset)	45K	0.597	0.335
FBIS-22M (subset)	150K	0.678	0.429
FBIS-22M	636K	0.720	0.477

5.2. Operational Deployment

We evaluated the viability of the Delineate Anything model and the proposed post-processing workflow for solving the field delineation task at a national scale.

For this purpose, we generated a field delineation layer of Ukraine for 2024 using interpolated 5m and 2.5m spatial resolution Sentinel-2 imagery. Ukraine, with an area of 603,000 km², presents substantial challenges for scalable solutions. In addition to its size, the country features considerable agricultural diversity, ranging from large, contiguous plots to extremely fragmented micro-fields. This heterogeneity adds complexity to the delineation task, making accurate boundary extraction more difficult, while simultaneously offering a rigorous testbed for evaluating model robustness across real-world scenarios.

Using a consumer-grade desktop equipped with an AMD Ryzen 9 9900X 12-Core CPU, NVIDIA GeForce RTX 5070 Ti 16GB GPU, and 64GB of RAM, the full map was produced in 5.4 hours (excluding data acquisition time, for 5 m data).

Considering that Ukraine is one of the largest countries in Europe, this result demonstrates the scalability of our approach and its potential applicability at the continental or global scale.

The input Sentinel-2 composite and the resulting field delineation output are shown in Figure 11.

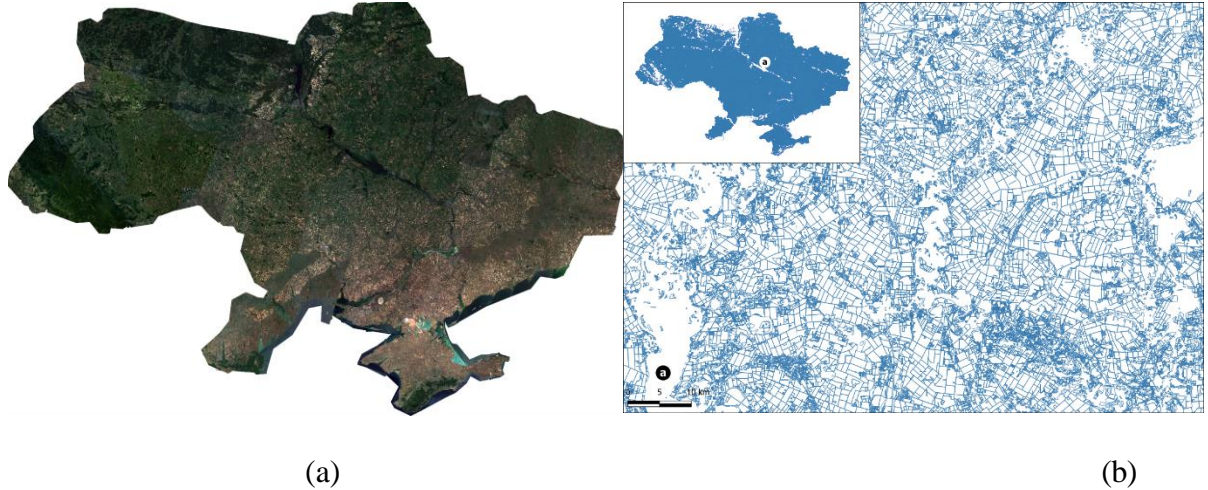


Figure 11: (a) - input Sentinel-2 composite; (b) - output vector fields.

We compared our results with those obtained by Sinergise Solutions (2024) and NASA Harvest (2023).

Figure 12 illustrates the distribution of detected fields larger than 0.25 hectares. This threshold corresponds to the practical lower limit of what can be reliably delineated from Sentinel-2 imagery (approximately 25 pixels per field).

Our method detected 3.75 million fields using interpolated 5m data and 5.15 million fields with 2.5m data. For comparison, Sinergise Solutions detected 2.66 million fields, and NASA Harvest identified 1.69 million based on 2023 data.

Figure 12 also shows that our method produces a higher number of excessively large fields, ranging from 1,000 to 10,000 hectares (3-4 in log scale), which are absent in the other products. Conversely, our method detects a significantly larger number of fields in the 1 to 10 hectares range. At the same time, utilization of 2.5m data greatly increases detection of small fields in the 0.25-1 ha range. However, over-detection of large fields and longer delineation time make the 2.5m version of the map impractical.

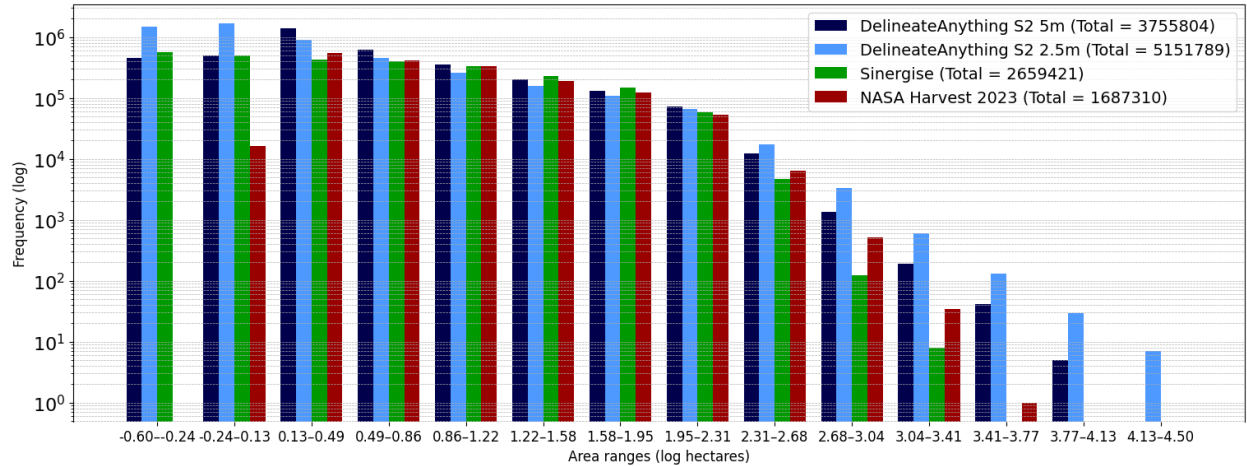


Figure 12: Log-log distribution of detected field sizes by different delineation products.

Figure 13 shows a comparison of delineations of four regions with an area of approximately 7 km². The Delineate Anything approach on 5m data consistently detects small private fields more effectively than competing methods. In contrast, the Sinergise Solution product captures only a portion of these parcels, while NASA Harvest fails to detect them altogether. For medium-sized fields, Delineate Anything and Sinergise Solutions recognize fields with similar efficiency and generally have better coverage compared to NASA Harvest.

Unlike Sinergise Solutions, which applies a buffering step, the fields delineated by Delineate Anything more accurately reflect their true extent, making them better suited for downstream analyses that require precise area estimates.

A broader side-by-side visual comparison of delineation results across multiple regions is available in Supplementary Video 1 (Figure 14).

Note for print readers: Supplementary Video 1 demonstrates side-by-side results from Delineate Anything, Sinergise Solutions, and NASA Harvest across several diverse regions. It highlights improved detection of small fields and better delineation of medium-sized ones.

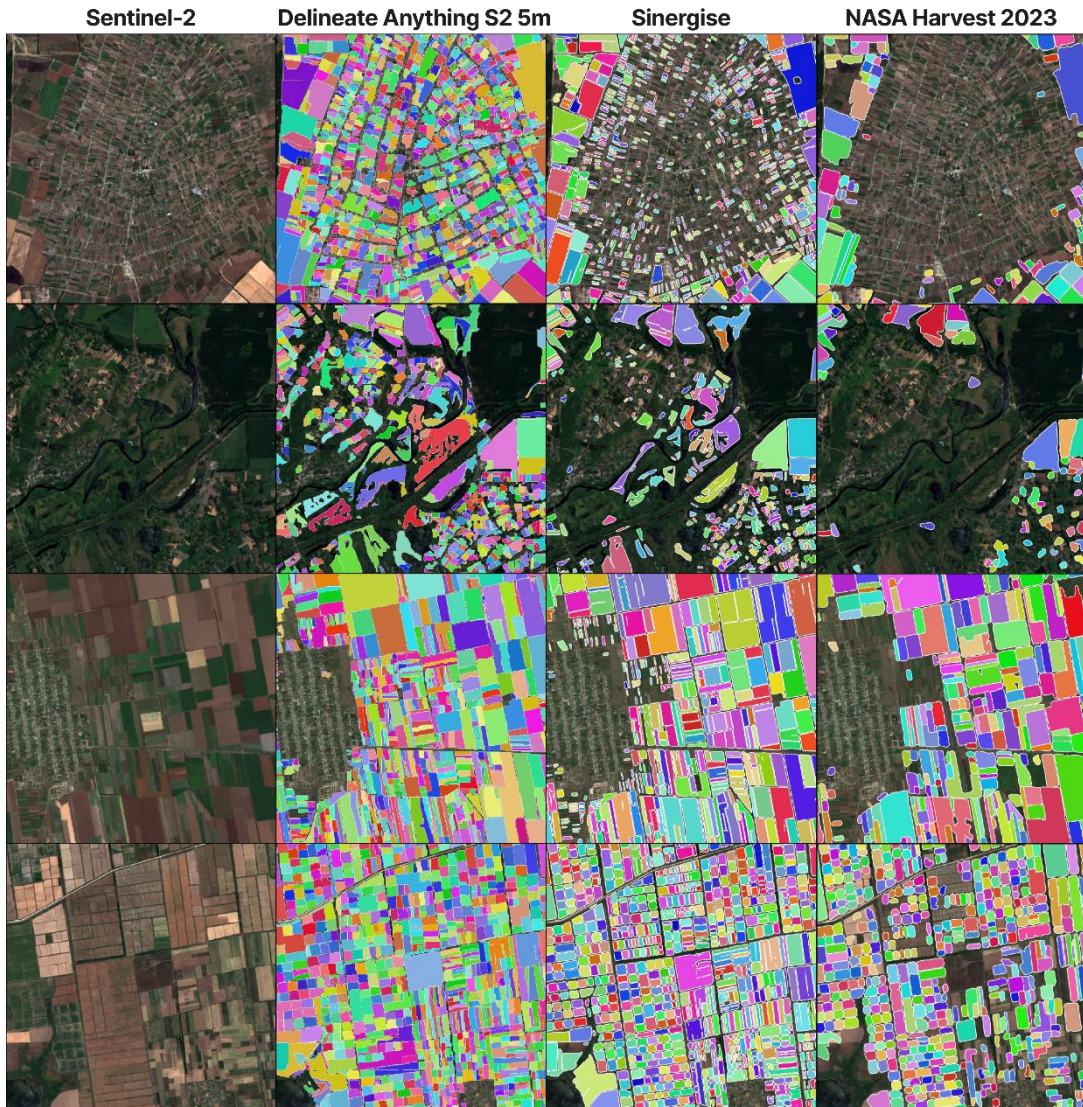


Figure 13: Comparison of field delineations from different products across four 7 km^2 regions.

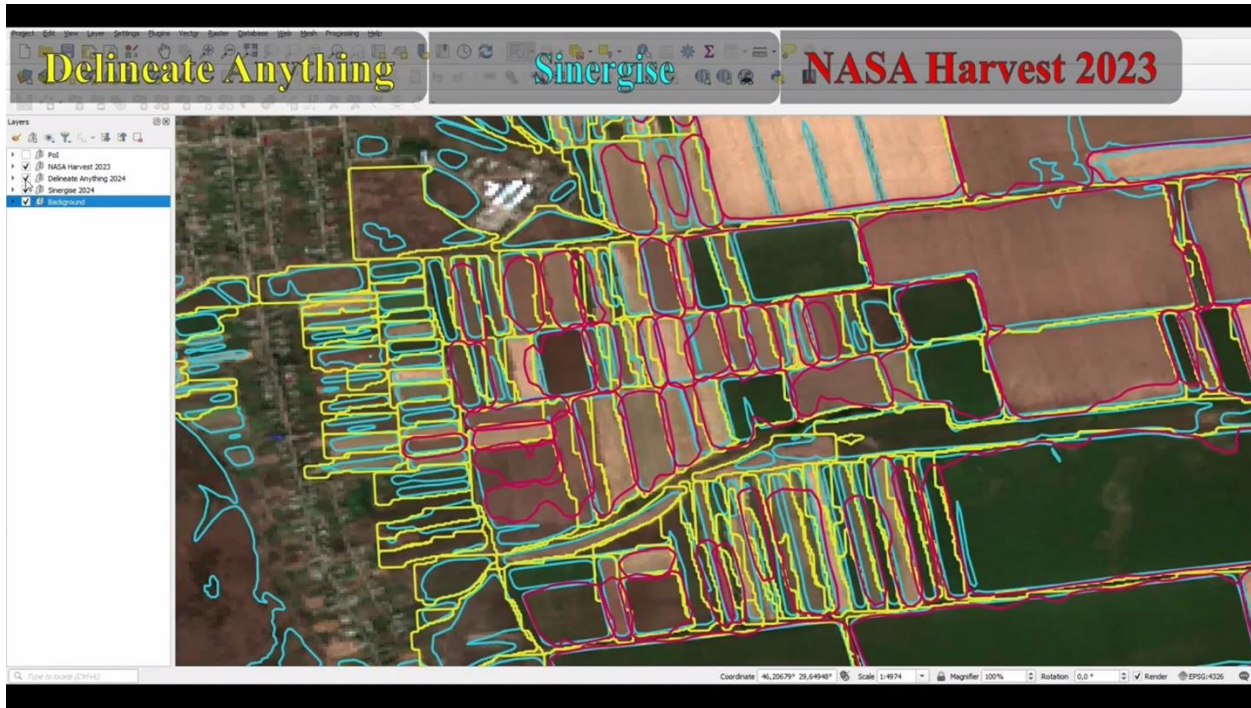


Figure 14: Supplementary Video 1: Comparative delineation results across several regions using Delineate Anything (5 m), Sinergise Solutions (2024), and NASA Harvest (2023). Delineate Anything shows improved detection of small private fields and more accurate geometry of medium-sized parcels.

6. Discussion

6.1. Methodological advances in field delineation

The results of this study demonstrate that reformulating field boundary delineation as an instance segmentation problem can substantially improve both accuracy and scalability compared to conventional semantic segmentation approaches. At the core of this advancement is the Delineate Anything (DelAny) model, which was trained on the large-scale, multi-resolution FBIS-22M dataset. DelAny achieves state-of-the-art mean Average Precision (mAP) at multiple Intersection-over-Union (IoU) thresholds and delivers inference speeds up to 400 \times faster than

foundation models such as SAM2. These improvements directly address persistent shortcomings of existing methods, which frequently generate merged parcels and incomplete boundaries, reducing the utility of automated outputs for cadastral, policy, and agricultural monitoring applications.

Building on the DelAny model, the broader DelAnyFlow methodology introduces a modular, resolution-agnostic framework that integrates the instance segmentation outputs with a structured set of post-processing, merging, mosaicking, and vectorization procedures. This design enables the generation of topologically consistent, non-overlapping field boundary layers that are fully analysis-ready. A key methodological advance of DelAnyFlow is the ability to seamlessly ingest inputs from very high-resolution (0.25 m) commercial imagery through 10 m Sentinel-2 composites, supporting deployment across diverse agro-ecological contexts.

The performance of the DelAnyFlow methodology, underpinned by the DelAny model, was consistently strong across diverse agricultural landscapes, including smallholder systems, large industrial fields, and heterogeneous mixed-use mosaics. On the FBIS-22M test set, DelAnyFlow achieved the highest mAP scores among all evaluated methods, while maintaining full topological consistency and analysis-readiness of outputs. Its ability to generalize across geographies and image resolutions—ranging from very-high-resolution (0.25 m) commercial imagery to medium-resolution (10 m) Sentinel-2 composites—demonstrates a level of robustness not achieved by existing approaches. These results confirm that instance-level training on a large, diverse dataset, when coupled with rigorous quality control, merging, and vectorization procedures, can effectively mitigate common errors such as field merging, boundary gaps, and topological inconsistencies.

By combining high segmentation accuracy with scalable processing and robust output integration, DelAnyFlow represents a significant step forward in operational field boundary mapping. Its performance meets the quality standards required for applications in agricultural monitoring, cadastral updates, and food security assessments, positioning it as a practical solution for national- and global-scale agricultural intelligence initiatives.

6.2. Comparison with existing approaches and products

Our results consistently outperform state-of-the-art models (SAM, SAM2, MultiTLF) in both object-level metrics and qualitative assessments across multiple regions. Notably, the improvement over SAM2 (88.5% in mAP@0.5 and 103% in mAP@0.5:0.95) indicates that foundation models pre-trained on natural images remain suboptimal for agricultural field delineation unless extensively adapted.

Comparison with operational products from Sinergise Solutions and NASA Harvest shows that DelAnyFlow identifies substantially more fields, particularly in the 1–10 ha size range, which is crucial for monitoring smallholder agriculture and fragmented agro-ecological systems.

6.3. Limitations and sources of uncertainty

Although DelAny generalizes well to unseen geographies in a zero-shot setting, quantitative evaluation outside Europe remains limited. The current FBIS-22M dataset is dominated by European agricultural landscapes, which may bias the model toward temperate, high-input systems. Transferability to highly heterogeneous smallholder systems (e.g., sub-Saharan Africa, Southeast Asia) requires further testing with annotated data from those regions.

Another limitation is the reliance on single-date optical imagery for the primary experiments. Although the post-processing chain filters non-agricultural classes, cloud contamination and phenological variations can still induce false boundaries. Temporal composites or the integration of multi-modal data (e.g., SAR) could further enhance robustness, particularly in persistently cloudy regions.

In some cases, especially where spectral boundaries between adjacent fields are weak or ambiguous, DelAnyFlow may produce larger-than-expected field polygons (>1000 ha). This could reflect a degree of over-aggregation in sparsely bounded areas. While the instance segmentation approach improves completeness, especially for small and fragmented fields, future work could explore additional constraints or refinement steps to better control generalization in such conditions.

6.4. Implications for agricultural monitoring and policy

The proposed field boundary delineation approach is particularly valuable for countries and regions where official cadastral data or LPIS layers are unavailable or incomplete, such as Ukraine, EU neighboring countries, and many nations in Africa. While the accuracy requirements of the EU LPIS protocols cannot be met with this method, as LPIS relies on orthophoto aerial imagery at very high spatial resolution and strict quality standards, the outputs generated by our workflow can serve as a valuable prototype in contexts without digital cadasters. This is particularly relevant for countries in the World's developing regions, and other regions where land parcel information is often fragmented or absent.

Field boundaries derived from satellite imagery can substantially improve the accuracy of crop type classification. They have also been applied in conflict settings to assess damage to

agricultural fields (Kussul et al., 2023) and to support broader environmental governance programs (Hall et al., 2021). By enabling the aggregation of spectral, meteorological, and vegetation indicators at the field level, classification algorithms can overcome the limitations of pixel-based approaches, which tend to perform poorly for small and irregularly shaped fields with minor crops. This benefit is critical for regions with highly fragmented agricultural landscapes, where averaging indicators across field polygons provides more robust and interpretable inputs for crop mapping and yield estimation.

In addition, automatically generated boundary layers can support agricultural statistics and tax monitoring. By identifying the location and size distribution of farms, governments and institutions can better distinguish smallholder plots from large agricultural holdings, which is valuable for assessing the structure of the agricultural sector and designing targeted policies. Such capabilities are particularly important for developing countries where cadastral systems are under development and reliable data on farm structure is lacking.

Finally, these boundary maps can serve as a foundation for a variety of agricultural monitoring tasks, including estimating cultivated area, supporting input subsidy programs, and identifying land use change over time. While not a replacement for official cadastral products, the proposed delineation approach provides a scalable and cost-effective means to fill critical data gaps in regions where field boundary information is otherwise unavailable.

6.5. Future research directions

Future research should focus on several complementary directions to further advance the accuracy and operational value of field boundary delineation. First, expanding the FBIS-22M dataset with annotated data from Africa, Asia, and South America will improve the model's robustness in

smallholder and mixed land-use systems that are currently underrepresented. Integrating multi-temporal optical imagery with synthetic aperture radar (SAR) data and other modalities could help resolve boundaries in cloudy regions and in fields with subtle spectral differences. Another important avenue is the incorporation of uncertainty quantification techniques so that confidence levels can be assigned to delineated boundaries, enabling users to better prioritize manual validation. Improvements in the adaptive post-processing stage, particularly by tuning area-based filtering and merging thresholds based on local agro-ecological conditions, could help reduce errors such as the over-aggregation of very large fields. Finally, operationalizing the workflow through cloud-native implementations and standardized APIs would facilitate adoption by national mapping agencies, agricultural ministries, and international monitoring initiatives, making large-scale, high-resolution field boundary mapping accessible to a wider range of end-users.

7. Conclusion

This study presented the DelAnyFlow, a resolution-agnostic instance segmentation methodology that produces accurate and topologically consistent agricultural field boundary layers from multi-resolution satellite imagery. DelAnyFlow significantly improves boundary completeness and quality compared to existing methods, generalizes effectively to unseen geographies, and is capable of generating national-scale outputs within hours on modest computing infrastructure.

The workflow's performance and scalability make it a practical tool for operational agricultural monitoring and policy-relevant applications. By enabling accurate field boundary delineation in regions lacking cadastral data, DelAny can support improved crop type classification, agricultural statistics, food security assessments, and monitoring of land-use change.

Its compatibility with multi-source optical data allows adoption in both smallholder and large-scale agricultural systems.

All trained models, source code, and derived field boundary layers are publicly available, ensuring reproducibility and facilitating integration into international monitoring initiatives, including GEOGLAM, FAO-supported systems, and national agricultural statistics frameworks. Future work will focus on expanding geographic diversity in training data, incorporating SAR and multi-temporal information, and refining uncertainty estimation to further enhance robustness.

By delivering a scalable, cost-effective, and open-source workflow, this work provides the remote sensing community and operational agencies with a strong foundation for next-generation agricultural intelligence systems at regional to global scales.

Acknowledgements

This work was partially supported by the European Space Agency (ESA), the European Commission through the joint World Bank/EU project ‘Supporting Transparent Land Governance in Ukraine’ [grant numbers ENI/2017/387-093 and ENI/2020/418-654], expert contracts EC Joint Research Center (JRC) [CT-EX2022D670387-101, CT-EX2022D670387-102], National Research Foundation of Ukraine project “Geospatial monitoring system for the war impact on the agriculture of Ukraine based on satellite data” [grant number 2023.04/0039] (development and validation of field boundary datasets for war-affected areas), “DT4LC: Developing Scalable Digital Twin Models for Land Cover Change Detection Using Machine Learning” [grant number 2023.01/0040] (development and validation of training data representing land cover and land use changes under climate-driven and management-driven transformations), and NASA Grants 80NSSC24K0354 and 80NSSC23M0032.

We also gratefully acknowledge Sinergise Solutions (<https://sinergise.com>) and NASA Harvest (<https://nasaharvest.org>) for providing access to their field boundary datasets for Ukraine, which were essential for comparative evaluation.

Finally, we express our gratitude to Senior Researcher of the Space Research Institute NASU-SSAU, Dr. Bohdan Yailymov, for his significant contribution to the automated formation of the FBIS-22M dataset.

Data availability

A project landing page is available at: <https://lavreniuk.github.io/Delineate-Anything/>.

The Delineate Anything model, along with training scripts, pre-trained weights, and the DelAnyFlow inference pipeline, is publicly available at: <https://github.com/Lavreniuk/Delineate-Anything>.

A public demonstration of national-scale field boundaries for Ukraine in the 2024 season, generated using Sentinel-2 imagery and the proposed model, is accessible at: <https://delineate-anything.projects.earthengine.app/view/ua2024fields>.

A subset of the FBIS-22M dataset introduced in this work is available for research purposes: <https://huggingface.co/datasets/MykolaL/FBIS-22M>.

References

Aung, H.L., Uzkent, B., Burke, M., Lobell, D., Ermon, S., 2020. Farm parcel delineation using spatio-temporal convolutional networks. IEEE Computer Society Conference on Computer Vision and Pattern Recognition Workshops 2020-June, 340–349.
doi:10.1109/CVPRW50498.2020.00046.

Bertasius, G., Shi, J., Torresani, L., 2014. Deepedge: A multi-scale bifurcated deep network for top-down contour detection. Proceedings of the IEEE Computer Society Conference on Computer Vision and Pattern Recognition 07-12-June-2015, 4380–4389. doi:10.1109/CVPR.2015.7299067.

Cambrin, D.R., Poeta, E., Pastor, E., Cerquitelli, T., Baralis, E., Garza, P., 2024. Kan you see it? kans and sentinel for effective and explainable crop field segmentation. Lecture Notes in Computer Science 15625 LNCS, 115–131. doi:10.1007/978-3-031-91835-3_8.

Chen, K., Liu, C., Chen, H., Zhang, H., Li, W., Zou, Z., Shi, Z., 2024. Rsprompter: Learning to prompt for remote sensing instance segmentation based on visual foundation model. IEEE Transactions on Geoscience and Remote Sensing 62, 1–17. doi:10.1109/TGRS.2024.3356074.

Chen, Z., Deng, L., Luo, Y., Li, D., Junior, J.M., Gonçalves, W.N., Nurunnabi, A.A.M., Li, J., Wang, C., Li, D., 2022a. Road extraction in remote sensing data: A survey. International Journal of Applied Earth Observation and Geoinformation 112, 102833. doi:10.1016/J.JAG.2022.102833.

Chen, Z., Duan, Y., Wang, W., He, J., Lu, T., Dai, J., Qiao, Y., 2022b. Vision transformer adapter for dense predictions. 11th International Conference on Learning Representations, ICLR 2023. doi:10.48550/ARXIV.2205.08534.

Crommelinck, S., Bennett, R., Gerke, M., Nex, F., Yang, M.Y., Vosselman, G., 2016. Review of automatic feature extraction from high-resolution optical sensor data for uav-based cadastral mapping. Remote Sensing 2016, Vol. 8, Page 689 8, 689. doi:10.3390/RS8080689.

D'Andrimont, R., Claverie, M., Kempeneers, P., Muraro, D., Yordanov, M., Peressutti, D., Batič, M., Waldner, F., 2023. Ai4boundaries: an open ai-ready dataset to map field boundaries with sentinel-2 and aerial photography. *Earth System Science Data* 15, 317–329. doi:10.5194/ESSD-15-317-2023.

Diakogiannis, F.I., Waldner, F., Caccetta, P., Wu, C., 2020. Resunet-a: A deep learning framework for semantic segmentation of remotely sensed data. *ISPRS Journal of Photogrammetry and Remote Sensing* 162, 94–114. doi:10.1016/J.ISPRSJPRS.2020.01.013.

Du, Z., Yang, J., Ou, C., Zhang, T., 2019. Smallholder crop area mapped with a semantic segmentation deep learning method. *Remote Sensing* 2019, Vol. 11, Page 888 11, 888. doi:10.3390/RS11070888.

Duvvuri, S., Kambhammettu, B.P., 2023. Hs-frag: An open source hybrid segmentation tool to delineate agricultural fields in fragmented landscapes. *Computers and Electronics in Agriculture* 204, 107523. doi:10.1016/J.COMPAG.2022.107523.

Erden, H., Aslan, M., Özcanli, C.B., 2015. To establish a new subsidy system. 2015 4th International Conference on Agro-Geoinformatics, Agro-Geoinformatics 2015 , 57–60. doi:10.1109/AGRO-GEOINFORMATICS.2015.7248142.

Fang, Y., Wang, W., Xie, B., Sun, Q., Wu, L., Wang, X., Huang, T., Wang, X., Cao, Y., 2022. Eva: Exploring the limits of masked visual representation learning at scale. *Proceedings of the IEEE Computer Society Conference on Computer Vision and Pattern Recognition* 2023-June, 19358–19369. doi:10.1109/CVPR52729.2023.01855.

Garcia-Pedrero, A., Lillo-Saavedra, M., Rodriguez-Esparragon, D., Gonzalo-Martin, C., 2019. Deep learning for automatic outlining agricultural parcels: Exploiting the land parcel

identification system. IEEE Access 7, 158223–158236.

doi:10.1109/ACCESS.2019.2950371.

Garnot, V.S.F., Landrieu, L., 2021. Panoptic segmentation of satellite image time series with convolutional temporal attention networks. Proceedings of the IEEE International Conference on Computer Vision , 4852–4861. doi:10. 1109/ICCV48922.2021.00483.

Garnot, V.S.F., Landrieu, L., Chehata, N., 2022. Multi-modal temporal attention models for crop mapping from satellite time series. ISPRS Journal of Photogrammetry and Remote Sensing 187, 294–305. doi:10.1016/J.ISPRSJPRS.2022.03.012.

Gopidas, D.K., Priya, D.R., 2022. Hybrid segmentation method for boundary delineation of agricultural fields in multitemporal satellite image using hs-psp-fcnn. Materials Today: Proceedings 51, 2272–2276. DOI:10.1016/J.MATPR.2021.11.397.

Graesser, J., Ramankutty, N., 2017. Detection of cropland field parcels from landsat imagery. Remote Sensing of Environment 201, 165–180. doi:10.1016/J.RSE.2017.08.027.

Hall, J.V., Zibtsev, S.V., Giglio, L., Skakun, S., Myroniuk, V., Zhuravel, O., ... & Kussul, N., 2021. Environmental and political implications of underestimated cropland burning in Ukraine. *Environmental Research Letters*, 16(6), 064019. DOI: 10.1088/1748-9326/abfc04.

Huang, Z., Jing, H., Liu, Y., Yang, X., Wang, Z., Liu, X., Gao, K., Luo, H., 2024. Segment anything model combined with multi-scale segmentation for extracting complex cultivated land parcels in high-resolution remote sensing images. Remote Sensing 2024, Vol. 16, Page 3489 16, 3489. doi:10.3390/RS16183489.

Kang, Y., Özdogan, M., 2019. Field-level crop yield mapping with landsat using a hierarchical data assimilation approach. *Remote Sensing of Environment* 228, 144–163. doi:10.1016/J.RSE.2019.04.005.

Kerner, H., Chaudhari, S., Ghosh, A., Robinson, C., Ahmad, A., Choi, E., Jacobs, N., Holmes, C., Mohr, M., Dodhia, R., Ferres, J.M.L., Marcus, J., 2024a. Fields of the world: A machine learning benchmark dataset for global agricultural field boundary segmentation. *Proceedings of the AAAI Conference on Artificial Intelligence* 39, 28151–28159. doi:10.1609/aaai.v39i27.35034.

Kerner, H., Sundar, S., Satish, M., 2024b. Multi-region transfer learning for segmentation of crop field boundaries in satellite images with limited labels. *arXiv preprint arXiv:2404.00179*. doi:10.48550/ARXIV.2404.00179.

Khanam, R., Hussain, M., 2024. Yolov11: An overview of the key architectural enhancements. *arXiv preprint arXiv:2410.17725*. doi:10.48550/ARXIV.2410.17725.

Kirillov, A., Mintun, E., Ravi, N., Mao, H., Rolland, C., Gustafson, L., Xiao, T., Whitehead, S., Berg, A.C., Lo, W.Y., Dollár, P., Girshick, R., 2023. Segment anything. *Proceedings of the IEEE International Conference on Computer Vision*, 3992–4003. doi:10.1109/ICCV51070.2023.00371.

Kussul, N., Kolotii, A., Shelestov, A., Yailymov, B., Lavreniuk, M., 2017. Land degradation estimation from global and national satellite-based datasets within UN program. In: 2017 9th IEEE International Conference on Intelligent Data Acquisition and Advanced Computing Systems: Technology and Applications (IDAACS). IEEE, Vol. 1, pp. 383–386. DOI: 10.1109/IDAACS.2017.8095109.

Kussul, N., Drozd, S., Yailymova, H., Shelestov, A., Lemoine, G., Deininger, K., 2023. Assessing damage to agricultural fields from military actions in Ukraine: An integrated approach using statistical indicators and machine learning. *International Journal of Applied Earth Observation and Geoinformation* 125, 103562. [doi:10.1016/j.jag.2023.103562](https://doi.org/10.1016/j.jag.2023.103562).

Kuznetsova, A., Rom, H., Alldrin, N., Uijlings, J., Krasin, I., Pont-Tuset, J., Kamali, S., Popov, S., Malloci, M., Kolesnikov, A., Duerig, T., Ferrari, V., 2020. The open images dataset v4: Unified image classification, object detection, and visual relationship detection at scale. *International Journal of Computer Vision* 128, 1956–1981. doi:10.1007/s11263-020-01316-z.

Lavreniuk, M., Kussul, N., Novikov, A., 2018. Deep learning crop classification approach based on sparse coding of time series of satellite data. In: *IGARSS 2018 - 2018 IEEE International Geoscience and Remote Sensing Symposium*. IEEE, pp. 4812–4815. DOI: 10.1109/IGARSS.2018.8518263.

Lavreniuk, M., 2024. Spidepth: Strengthened pose information for self-supervised monocular depth estimation. *arXiv preprint arXiv:2404.12501*.doi:10.48550/ARXIV.2404.12501.

Lavreniuk, M., Bhat, S.F., Müller, M., Wonka, P., 2025a. Evp: Enhanced visual perception using inverse multi-attentive feature refinement and regularized image-text alignment. *Lecture Notes in Computer Science* 15623 LNCS, 206–225. doi:10.1007/978-3-031-91569-7_14.

Lavreniuk, M., Kussul, N., Shelestov, A., Yailymov, B., Salii, Y., Kuzin, V., Szantoi, Z., 2025b. Delineate anything: Resolution-agnostic field boundary delineation on satellite imagery. *arXiv preprint arXiv:2504.02534*. doi:10.48550/ARXIV.2504.02534.

Li, T., Johansen, K., McCabe, M.F., 2022. A machine learning approach for identifying and delineating agricultural fields and their multi- temporal dynamics using three decades of

landsat data. *ISPRS Journal of Photogrammetry and Remote Sensing* 186, 83–101. doi:10.1016/J.ISPRSJPRS.2022.02.002.

Lin, T.Y., Maire, M., Belongie, S., Hays, J., Perona, P., Ramanan, D., Dollár, P., Zitnick, C.L., 2014. Microsoft coco: Common objects in context. *Lecture Notes in Computer Science (including subseries Lecture Notes in Artificial Intelligence and Lecture Notes in Bioinformatics)* 8693 LNCS, 740–755. doi:10.1007/978-3-319-10602-1_48.

Liu, S., Liu, L., Xu, F., Chen, J., Yuan, Y., Chen, X., 2022. A deep learning method for individual arable field (iaf) extraction with cross- domain adversarial capability. *Computers and Electronics in Agriculture* 203, 107473. doi:10.1016/J.COMPAG.2022.107473.

Liu, Y., Cheng, M.M., Hu, X., Wang, K., Bai, X., 2019. Richer convolutional features for edge detection. *IEEE Transactions on Pattern Analysis and Machine Intelligence* 41, 1939–1946. doi:10.1109/TPAMI.2018.2878849.

Lu, R., Wang, N., Zhang, Y., Lin, Y., Wu, W., Shi, Z., 2022. Extraction of agricultural fields via dasfnet with dual attention mechanism and multi-scale feature fusion in south xinjiang, china. *Remote Sensing* 2022, Vol. 14, Page 2253 14, 2253. doi:10.3390/RS14092253.

Lv, Y., Zhang, C., Yun, W., Gao, L., Wang, H., Ma, J., Li, H., Zhu, D., 2020. The delineation and grading of actual crop production units in modern smallholder areas using rs data and mask r-cnn. *Remote Sensing* 2020, Vol. 12, Page 1074 12, 1074. doi:10.3390/RS12071074.

Masoud, K.M., Persello, C., Tolpekin, V.A., 2019. Delineation of agricultural field boundaries from sentinel-2 images using a novel super-resolution contour detector based on fully convolutional networks. *Remote Sensing* 2020, Vol. 12, Page 59 12, 59. doi:10.3390/RS12010059.

North, H.C., Pairman, D., Belliss, S.E., 2019. Boundary delineation of agricultural fields in multitemporal satellite imagery. *IEEE Journal of Selected Topics in Applied Earth Observations and Remote Sensing* 12, 237–251. doi:10.1109/JSTARS.2018.2884513.

O'Connell, J., Bradter, U., Benton, T.G., 2015. Wide-area mapping of small-scale features in agricultural landscapes using airborne remote sensing. *ISPRS Journal of Photogrammetry and Remote Sensing* 109, 165–177. doi:10.1016/J.ISPRSJPRS.2015.09.007.

Osco, L.P., Wu, Q., de Lemos, E.L., Gonçalves, W.N., Ramos, A.P.M., Li, J., Marcato, J., 2023. The segment anything model (sam) for remote sensing applications: From zero to one shot. *International Journal of Applied Earth Observation and Geoinformation* 124. doi:10.1016/j.jag.2023.103540.

Persello, C., Member, S., Grift, J., Fan, X., Paris, C., Hänsch, R., Koeva, M., Nelson, A., 2023. Ai4smallfarms: A dataset for crop field delineation in southeast asian smallholder farms. *IEEE GEOSCIENCE AND REMOTE SENSING LETTERS* 20, 2023. doi:10.17026/dans-xy6-ngg6.

Rahman, M.S., Di, L., Yu, E., Zhang, C., Mohiuddin, H., 2019. In-season major crop-type identification for us cropland from landsat images using crop-rotation pattern and progressive data classification. *Agriculture* 2019, Vol. 9, Page 17 9, 17. doi:10.3390/AGRICULTURE9010017.

Ravi, N., Gabeur, V., Hu, Y.T., Hu, R., Ryali, C., Ma, T., Khedr, H., Rädle, R., Rolland, C., Gustafson, L., Mintun, E., Pan, J., Alwala, K.V., Carion, N., Wu, C.Y., Girshick, R., Dollár, P., Feichtenhofer, C., Fair, M., 2024. Sam 2: Segment anything in images and videos. *arXiv preprint arXiv:2408.00714*. doi:10.48550/ARXIV.2408.00756.

Ren, S., Luzi, F., Lahrichi, S., Kassaw, K., Collins, L.M., Bradbury, K., Malof, J.M., 2023. Segment anything, from space? Proceedings - 2024 IEEE Winter Conference on Applications of Computer Vision, WACV 2024 , 8340–8350. doi:10.1109/WACV57701.2024.00817.

Sadeh, Y., Wagner, J., Nair, S.S., Oliynyk, O., Belles, E., Bibih, A., D'Harboullé, L., Bendahmane, H., Gupta, M., Becker-Reshef, I., 2025. National-scale in-season field boundaries of ukraine using remote sensing. *Scientific Data* 12. doi:10.1038/S41597-025-05190-7.,

Schuhmann, C., Beaumont, R., Vencu, R., Gordon, C., Wightman, R., Cherti, M., Coombes, T., Katta, A., Mullis, C., Wortsman, M., Schramowski, P., Kundurthy, S., Crowson, K., Schmidt, L., Kaczmarczyk, R., Jitsev, J., 2022. Laion-5b: An open large-scale dataset for training next generation image-text models. *Advances in Neural Information Processing Systems* 35. doi:10.48550/ARXIV.2210.08402.

Seedz, R.F.R., Gaivota, V.N.L., Seedz, L.V.O., Seedz, A.F.C.B., Gaivota, W.S., Seedz, B.S.O., Seedz, M.N.B., 2024. A unified framework for cropland field boundary detection and segmentation. *Proceedings - 2024 IEEE Winter Conference on Applications of Computer Vision Workshops, WACVW 2024* , 636–644. doi:10.1109/WACVW60836.2024.00073.

Sun, J., Yan, S., Yao, X., Gao, B., Yang, J., 2024. A segment anything model based weakly supervised learning method for crop mapping using sentinel-2 time series images. *International Journal of Applied Earth Observation and Geoinformation* 133, 104085. doi:10.1016/J.JAG.2024.104085.

Tetteh, G.O., Schwieder, M., Erasmi, S., Conrad, C., Gocht, A., 2023. Comparison of an optimised multiresolution segmentation approach with deep neural networks for delineating agricultural fields from sentinel-2 images. *PFG - Journal of Photogrammetry, Remote*

Sensing and Geoinformation Science 91, 295–312. doi:10.1007/ S41064-023-00247-X/METRICS.

Tripathy, P., Baylis, K., Wu, K., Watson, J., Jiang, R., 2024. Investigating the segment anything foundation model for mapping smallholder agriculture field boundaries without training labels. arXiv preprint arXiv:2407.01846. doi:10.48550/ARXIV.2407.01846.

Turker, M., Kok, E.H., 2013. Field-based sub-boundary extraction from remote sensing imagery using perceptual grouping. ISPRS Journal of Photogrammetry and Remote Sensing 79, 106–121. doi:10.1016/J.ISPRSJPRS.2013.02.009.

van der Velden, D., Klerkx, L., Dessein, J., Debruyne, L., 2025. Governance by satellite: Remote sensing, bureaucrats and agency in the common agricultural policy of the european union. Journal of Rural Studies 114, 103558. doi:10.1016/J.JRURSTUD.2024.103558.

Wagner, M.P., Oppelt, N., 2020. Deep learning and adaptive graph-based growing contours for agricultural field extraction. Remote Sensing 2020, Vol. 12, Page 1990 12, 1990. doi:10.3390/RS12121990.

Waldner, F., Diakogiannis, F.I., 2020. Deep learning on edge: Extracting field boundaries from satellite images with a convolutional neural network. Remote Sensing of Environment 245, 111741. doi:10.1016/J.RSE.2020.111741.

Waldner, F., Diakogiannis, F.I., Batchelor, K., Ciccotosto-Camp, M., Cooper-Williams, E., Herrmann, C., Mata, G., Toovey, A., 2021. Detect, consolidate, delineate: Scalable mapping of field boundaries using satellite images. Remote Sensing 2021, Vol. 13, Page 2197 13, 2197. doi:10.3390/RS13112197.

Wang, A., Chen, H., Liu, L., Chen, K., Lin, Z., Han, J., Ding, G., 2024. Yolov10: Real-time end-to-end object detection. *Advances in Neural Information Processing Systems* 37. doi: 10.48550/ARXIV.2405.14458.

Wang, L., Fang, S., Li, R., Meng, X., 2022a. Building extraction with vision transformer. *IEEE Transactions on Geoscience and Remote Sensing* 60. doi:10.1109/TGRS.2022.3186634.

Wang, M., Wang, J., Cui, Y., Liu, J., Chen, L., 2022b. Agricultural field boundary delineation with satellite image segmentation for high-resolution crop mapping: A case study of rice paddy. *Agronomy* 2022, Vol. 12, Page 2342 12, 2342. doi:10.3390/AGRONOMY12102342.

Wang, S., Waldner, F., Lobell, D.B., 2022c. Unlocking large-scale crop field delineation in smallholder farming systems with transfer learning and weak supervision. *Remote Sensing* 2022, Vol. 14, Page 5738 14, 5738. doi:10.3390/RS14225738.

Watkins, B., van Niekerk, A., 2019. A comparison of object-based image analysis approaches for field boundary delineation using multi-temporal sentinel-2 imagery. *Computers and Electronics in Agriculture* 158, 294–302. doi:10.1016/J.COMPAG.2019.02.009.

Xie, D., Xu, H., Xiong, X., Liu, M., Hu, H., Xiong, M., Liu, L., 2023. Cropland extraction in southern china from very high-resolution images based on deep learning. *Remote Sensing* 2023, Vol. 15, Page 2231 15, 2231. doi:10.3390/RS15092231.

Xie, S., Tu, Z., 2015. Holistically-nested edge detection. *International Journal of Computer Vision* 125, 3–18. doi:10.1007/s11263-017-1004-z.

Xie, Y., Wu, H., Tong, H., Xiao, L., Zhou, W., Li, L., Wanger, T.C., 2025. fabsam: A farmland boundary delineation method based on the segment anything model. *arXiv preprint arXiv:2501.12487*. doi:10.48550/ARXIV.2501.12487.

Yan, L., Roy, D.P., 2014. Automated crop field extraction from multi-temporal web enabled landsat data. *Remote Sensing of Environment* 144, 42–64.
doi:10.1016/J.RSE.2014.01.006.

Zong, Z., Song, G., Liu, Y., 2023. Detrs with collaborative hybrid assignments training. doi: 10.48550/ARXIV.2211.12860.